Introducing: Double Renshaw-Haberman

by
Athinogenis-Alexandros Kostoulas
ANR 875753

A thesis submitted in partial fulfillment of the requirements for the degree of Master of Science in Quantitative Finance and Actuarial Science

Tilburg Schoolf of Economics and Management
Tilburg University

Supervised by:
dr. Jeroen Kerkhof (Tilburg University)
P.M. Bouwknegt(Nationale-Nederlanden)
T.E. Feenstra (Nationale-Nederlanden)

April 18, 2024

Contents

1 Acknowledgments

I am genuinely grateful to Prof. Jeroen Kerkhof for his guidance throughout my thesis journey. From beginning to end, he encouraged me to pursuit my research further and was always available to assist with the challenges that I faced. He is excellent to work with and, above, all a great person. I am truly thankful for the opportunity to have conducted my thesis under his supervision.

I would also like to extend my thanks to my supervisors at Nationale-Nederlanden, Pieter Bouwknegt and Thijs Feenstra, for trusting me with this fascinating project and for their support throughout my internship.

Last but not least, my heartfelt appreciation goes to my family and friends for their constant encouragement during this period of my life. Their belief in me and their presence were crucial in carrying out this project.

I would like to dedicate this thesis to the loving memory of my grandfather, Ioannis Kostoulas, who passed away this September.

2 Abstract

This thesis introduces the Double Renshaw-Haberman model as an innovative approach to mortality projections, particularly for the Dutch insurance sector. Focusing on the critical need for precise mortality forecasts amid demographic shifts, it evaluates the efficacy of age-period-cohort models, emphasizing the incorporation of cohort effects. An examination of the dynamics and the estimation process of the Lee-Carter model and its extensions is conducted in order to create space for qualitative and technical comparison. Through the comparative analysis, the research highlights the potential of the Double Renshaw-Haberman model to enhance the accuracy of mortality projections, thereby aiding insurers like Nationale-Nederlanden in refining premium structures and financial strategies.

3 Research Question

In an era marked by increasing life expectancy and shifting demographic patterns, the field of actuarial science confronts a pressing challenge - effectively managing mortality risk. In this landscape, the demand for precise mortality projections has reached an unprecedented level of importance.

Mortality risk, intricately interwoven with longevity risk, serves as the cornerstone of actuarial assessments for insurers. Accurate mortality projections dictate pricing, risk assessment, and the long-term financial health of insurance companies. For Nationale-Nederlanden, an insurer entrusted with safeguarding the financial futures of countless policyholders, the implications of effective mortality projections are profound. Precise projections empower the company to make informed decisions regarding premium structures, reserves, and investment strategies, all of which significantly influence the insurer's competitiveness and ability to meet its obligations.

Life insurers and pension funds stand at the forefront of addressing this challenge. The prevailing mortality projection model utilized by Dutch life insurers follows an extension to the classical Lee-Carter model, the Li-Lee model, which assumes a constant age-specific response to the passage of time. However, it has not escaped criticism that this model, as noted by Lee and Miller in 2001, can often err on the side of underpredicting life expectancy. Given these concerns, this thesis embarks on a journey to assess:

> Could an age-period-cohort model offer a more accurate alternative for mortality projections in Dutch society?

To thoroughly address this research question, the thesis will unfold in several distinct phases. Firstly, an in-depth examination of the dynamics and methodology of the Lee-Carter model, introduced by Lee and Carter in 1992, will be undertaken. This will pave the way for an exploration of its extension, the Li-Lee model by Lee and Li in 2005 that is being employed by AG, thereby laying the foundation for subsequent comparative analyses. In parallel, an extensive review of existing literature will be conducted, focusing on models that have successfully incorporated the cohort effect, as exemplified by Renshaw and Haberman in 2006. This comprehensive literature review will serve as a crucial foundation for evaluating whether such cohort-incorporating models could offer a more efficient and accurate alternative for mortality projections, especially in the context of Dutch life insurers like Nationale-Nederlanden. Last, the Double Renshaw-Haberman model is going to be introduced and its performance is going to be evaluated with respect to its counterparts.

Furthermore, criticism of the Lee-Carter method has emerged due to its limited fit to historical data, hereby including its extension the Lee- Li model, particularly in countries where cohort effects have been observed in the past, as highlighted by Cairns (A. Cairns et al. 2007a). As a result, this thesis in order to shed light on the potential shortcomings of the current approach, seeks to investigate:

> Could similar cohort effects be detected in the Dutch mortality data-set?

Today's rapidly changing scenery has highlighted the importance of exploring new methods of producing accurate mortality predictions. Investigating the possibility of including cohort effects in the mortality models can be proven beneficial both for the life insurers and the policyholders. By incorporating cohort effects into their mortality models, life insurers can aim for more accurate predictions, which will enable them to achieve more precise pricing of policies. Insurers can avoid underpricing policies, which can lead to financial losses, and policyholders can benefit from more affordable premiums. In addition to improving pricing accuracy, incorporating cohort effects can also aid life insurers to better understand the factors that drive mortality rates. This can lead to more targeted interventions to improve policyholder health outcomes and further reduce mortality rates.

4 Literature Review

Compared to their ancestors, older people nowadays enjoy longer lifespans. In the past, when pension systems were first introduced, people expected to live only a few years after retirement. Some of them died before reaching the retirement age. But in the last century, life expectancy has improved significantly. A major accomplishment of contemporary societies is the marked improvement in the duration of life expectancy. However, the rising trend also creates huge difficulties to ensure solvency and profitability of longevity insurers and accurate pricing for the policy holders.

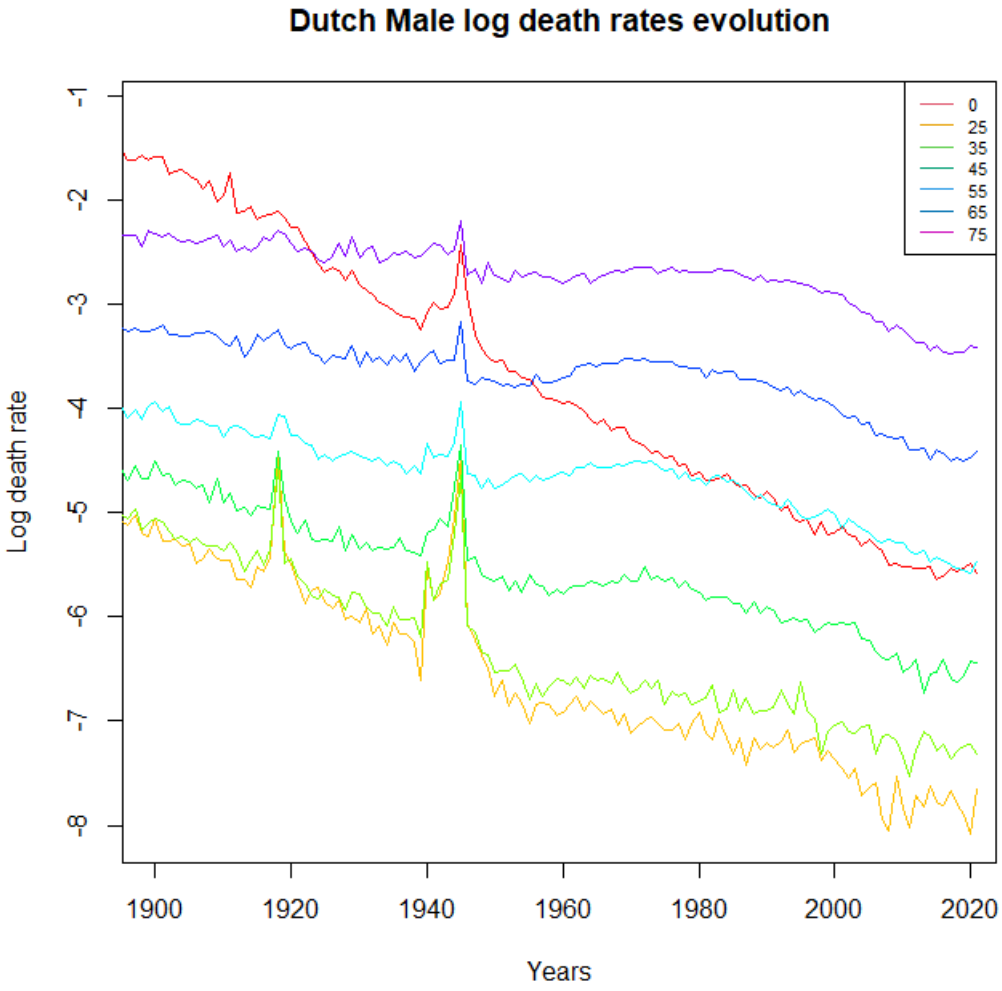

Figure 1: Evolution of log mortality rates in the Dutch male population over time for different ages.

Figure 1 shows that mortality differs strongly by age, with some ages changing more rapidly than others, e.g. infant mortality. Furthermore, it can be noted that the rate of decline by age shows tendency of stability throughout the years. However, it can be observed from Figure 1 that at some young adult ages the changes in mortality are irregular. It can be inferred that the slope of the lines that correspond to ages becomes less and less steep as the years advance. This refers to the fact that the medical advances and the general improvement of the living conditions have had a greater impact in the past than in the recent years.

Hence, the need of employing models that will aid in the accurate forecasting of mortality was created. As aforementioned the mortality models that will be explored in this thesis include the Lee-Carter, Li-Lee,

Renshaw-Haberman and AG models, and last the Double Renshaw-Haberman is going to be introduced. Although the main scope of this thesis is to compare the current mortality model in use by AG and a model that incorporates the cohort effect, such as DRH, it would be an omission not to discuss the model introduced by Lee and Carter in 1992 (Lee and Carter 1992). Since its publication, the Lee-Carter model stands as a benchmark for mortality projections and has served as a base for valuable extensions, such as the Li-Lee model (N. Li and Lee 2005a). The Lee-Carter model operates by utilising two age-specific constants and one time-varying index (H. Li, Zhou, and Ji 2023), which will be later on discussed in detail in Chapter 5. The components of the model originally are estimated from historical data from a single country, the U.S., and then are used to forecast future mortality rates by extrapolating the time trend and age-specific parameters. The model produces mortality forecasts based on the following formula:

$$\log(m_{x,t}) = \alpha_x + \beta_x \kappa_t + \epsilon_{x,t},$$

where x and t are the individual's current age and the current calendar year respectively. $m_{x,t}$ is the central death rate (see AppendixA), whereas α_x is the age-specific constant that captures the general shape of mortality by age. Additionally, β_x describes the relative speed of the change in mortality by age and κ_t is a one dimensional and time dependent process that quantifies the evolution of mortality over time (Stevens, De Waegenaere, and Melenberg 2011). The tendency of age-specif mortality rates to move together is reflected by $\beta_x \kappa_t$, whilst $\epsilon_{x,t}$ is the error term, with mean 0 and variance σ_ε^2 and indicates the age-specific historical influence that has been omitted by the model.

However, the Lee-Carter model has not escaped criticism, as the "assumption of constant age-specific response to the time index often leads to a constant rate of mortality improvement over time" (Bergeron-Boucher and Kjærgaard 2022). Thus, leading to an underprediction of the life expectancy for certain age groups and populations.

While the original Lee-Carter model relied on data from a single country, in 2005, Li and Lee proposed a strategy to enhance mortality forecasts within individual countries by drawing on the international context. The Li-Lee model, an extension of the traditional Lee-Carter model, considers data from multiple countries with shared socioeconomic characteristics. This approach aims to prevent cases of divergent mortality rate projections observed in the Lee-Carter model (N. Li and Lee 2005b), which are deemed highly unlikely. By employing a super-population model that forecasts mortality rates for a specific population, the model benefits from a larger dataset, allowing the detection of common patterns across a broader range of populations. This resulted in the following model introduced by Lee and Li:

$$\log(m_{x,t,i}) = \alpha_{x,i} + B_{x,i} K_{t,i} + \beta_{x,i} \kappa_{t,i} + \epsilon_{x,t,i},$$

where the terms of the formula have the same role as the classical Lee-Carter model, with an addition of the common factor $B_x K_t$.

In the Netherlands, the actuarial society known as the "Koninklijk Actuarieel Genootschap" (AG) utilizes the Li-Lee model for its mortality projections. According to the AG Projections Life Table 2022, this approach of incorporating mortality data from economically comparable nations is based on a dual rationale. First, there exists a positive correlation between prosperity and longevity (AG 2022). Secondly, these countries have consistently demonstrated an upward trajectory in period life expectancy over several decades. Therefore, by employing a broader European population with countries that closely resemble the Netherlands, the model can offer more accurate and robust forecasts for the long-term rise in the life expectancy for the Dutch population. Consequently, the AG selects only those countries that exhibit the greatest parallels with the Netherlands, in this case GDP serves as the primary measure of comparison, for inclusion in their version of the Li-Lee model. The extension of Li-Lee in use by AG is established as follows:

$$\log(m_{x,t}) = \log(m_{x,t}^{EU}) + \log(m_{x,t}^{NL}),$$

An additional critique directed to the Lee-Carter model pertains to its omission of cohort effects, a noteworthy factor influencing mortality dynamics. In 2006, Renshaw and Haberman introduced a model as an extension

to the Lee-Carter model by adding a new term that captures the cohort effect (Renshaw and Haberman 2006). The cohort effect is incorporated in the model and is expressed by the equation:

$$\log(m_{x,t}) = \alpha_x + \beta_x^1 \kappa_t^1 + \beta_x^0 \boldsymbol{\iota_{t-x}}$$

The cohorts are defined as the difference between the year of the individual's death and the individual's age at the time of death. Consequently, members of the cohort are grouped together and their mortality patterns are tracked over time. The motivation behind the cohort-based approach lies in the fact that cohorts may share comparable experiences and susceptibilities to external factors, such as advancement of medicine, raised awareness of prevention, smoking etc., which can later on influence their mortality projection. In Figure 2 the effect of cohort can be observed. The grouped 5-year populations depicted will move jointly as time passes. For instance, the cohort of 45-49 aged men will come in place of the 50-54 aged men cohort and will represent a smaller percentage of the total population.

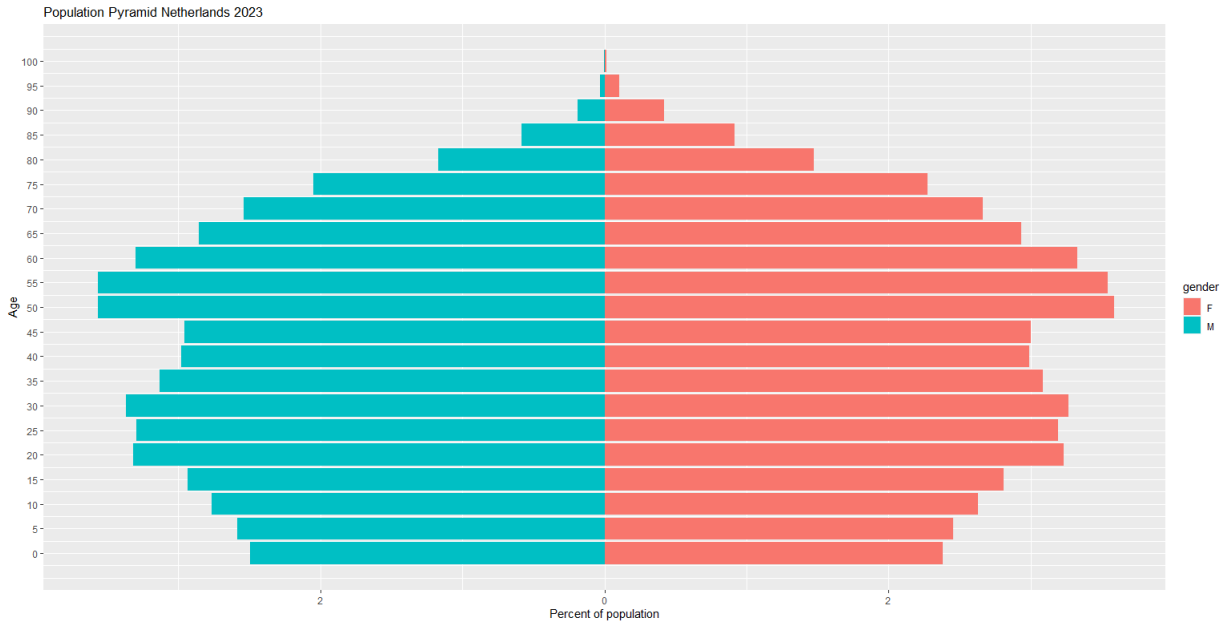

Figure 2: Population Pyramid that depicts the population distribution in the Netherlands over 1-year cohorts. Data obtained from CBS.

In 2002 (Brouhns, Denuit, and Vermunt 2002) presented a new method for constructing projected lifetables, an extension to the Lee-Carter model, using a Poisson log-bilinear regression approach. The article discusses the limitations of the traditional Lee-Carter model, namely the unrealistic assumption of normally distributed error terms. The variability of the logarithm of the observed force of mortality is greater at older ages compared to younger ages, due to the significantly smaller absolute number of deaths among older individuals, as can be seen in Figure 3 and Figure 4. The above led to the consideration of :

$$\mathrm{D}_{x,t} = \mathrm{Poisson}(\mathrm{E}_{x,t} e^{\alpha_x + \beta_x \kappa_t}),$$

where $D_{x,t}$ is the number of deaths in year t for the population aged x and $E_{x,t}$ is the exposure to risk, which can be interpreted as an estimate of the population, aged x, exposed to the risk of mortality during the calendar year t based on annual (January 1^{st}) population estimates.

Figure 3: Evolution of log death rates in the Dutch male population over age for the years depicted.

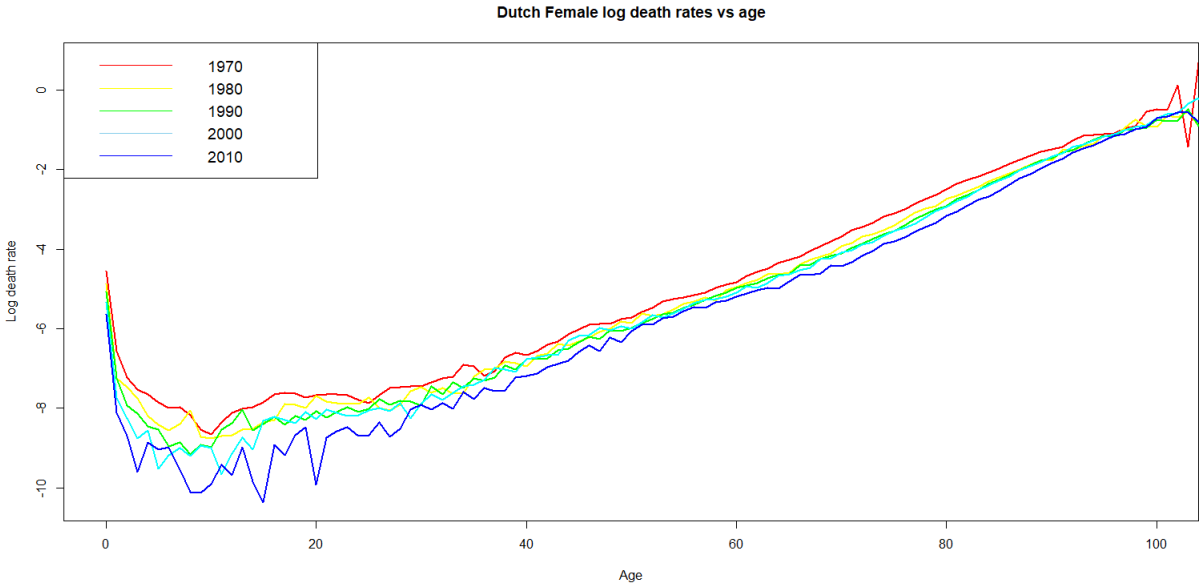

Figure 4: Evolution of log death rates in the Dutch female population over age for the years depicted.

It can be derived from both Figure 3 and Figure 4 that the log mortality rates for both males and females decreased, as the years passed. This can be attributed to raise of awareness of diseases, increase in vaccination, medical advances and a general adoption of a more healthy lifestyle. Furthermore, it is evident that mortality rates decrease at all ages with different "speeds". The reduction observed in the young ages can be accredited to the lessening of infant mortality. For both males and females the starting log death rates start relatively high and follow a decreasing trend until the age of 20. From then on, the lines follow a linear trend. It is worth noting that in the age of 20 a small hump can be observed, which appears bigger in the male figure and this can be attributed to accidental deaths.

5 Models

5.1 Lee-Carter model

5.1.1 Model Description

The model developed by Lee and Carter in 1992 is still nowadays widely used as a cornerstone in forecasting mortality rates and despite its simplicity it is proven to hold a very good performance and fit to the data (Lee 2000). A log-linear model fits to historical data on mortality rates for a given population, originally data on the US mortality, and assumes that mortality rates follow a log-linear trend with age and time, and that the age patterns of mortality rates remain constant over time.

The model assumes that the log of the age-specific mortality rates can be represented as a linear combination of a time-varying factor and an age-specific factor. The time-varying factor captures the overall trend in mortality rates over time, while the age-specific factor captures the variation in mortality rates by age.

The equation as introduced in the paper of Lee and Carter in 1992 :

$$\log(m_{x,t}) = \alpha_x + \beta_x \kappa_t + \epsilon_{x,t} \tag{1}$$

or alternatively:

$$m_{x,t} = e^{\alpha_x + \beta_x \kappa_t + \epsilon_{x,t}} \tag{2}$$

Lee and Carter propose forecasting the mortality index term κ_t by using a random walk with drift:

$$\kappa_t = \kappa_{t-1} + \theta + \epsilon_t, \tag{3}$$

where θ is the drift and the error term ϵ_t follows a normal distribution with mean 0 and variance σ_ϵ^2.

Many features of the Lee-Carter model make it a valuable tool for mortality rate predictions. First, the LC model is easy to understand and implement and particularly useful for cases with limited available data. Additionally, the model allows for easy interpretation of the factors that drive mortality rates, such as general trends in death rates and patterns of mortality unique to a given age. However, as a model it faces certain drawbacks, which should be considered in the mortality projection process. The model's assumption of linearity is one feature that has not escaped scrutiny. The Lee-Carter model assumes that mortality rates follow a log-linear trend with age and time, and that the age patterns of mortality rates remain constant over time. This assumption may not hold in all cases, particularly for populations that are experiencing rapid demographic or epidemiological changes.

It should be highlighted that the Lee-Carter approach solely makes use of historical data and makes no assumptions regarding future developments in the field of medicine or particular changes in the environment. Consequently, it is unable to forecast sudden improvements in mortality rates brought on by the development of medical treatments or cures, such as antibiotics. Similarly, the model cannot take into consideration future decline brought on by epidemics or the introduction of new illnesses, like the Spanish Influenza (1918) (black arrow) or wars like World War II (1945) (orange arrow). The two incident have been marked in Figure 5 and can be identified by the jumps in the evolution of the log death rates. Here, different age patterns can be observed, which are assumed away in the Lee-Carter model.

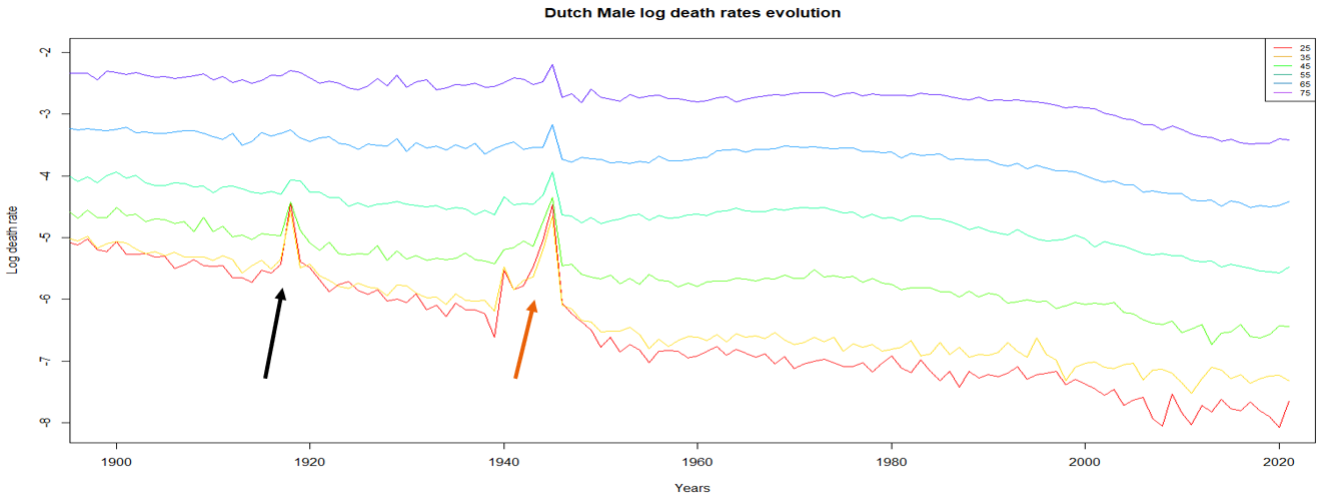

Figure 5: Evolution of log death rates in the Dutch male population over time for different ages and the benchmark of the Spanish Influenza (black) and World War II (orange). Regarding the former, it can be noted that young adult ages were affected more than older ages.

5.1.2 Estimating the parameters

Before one can utilize the Lee-Carter model to project mortality rates, the parameters must be estimated : α_x, β_x with $x = 1, 2, ..., N$ and κ_t with $t = 1, 2, ..., T$ and where the $\epsilon_{x,t}$, are homoskedastic centered error terms. The minimization

$$\sum_x \sum_t (\log(m_{x,t}) - \alpha_x - \beta_x \kappa_t)^2 \tag{4}$$

cannot work, since simple regression cannot be employed in order to fit the model described in 1, due to variables α_x, β_x and κ_t not being directly measurable. Following the original paper from Lee and Carter (1992), a Least Squares (LS) solution can be found using Singular Value Decomposition (SVD).

The model suffers from identification issues. Therefore, certain constraints must be applied in order to ensure identification, because a parameterization of the model's components :

$$(\alpha_x, \beta_x, \kappa_t) \hookrightarrow (\alpha_x, \frac{\beta_x}{c}, c \times \kappa_t) \tag{5}$$

$$(\alpha_x, \beta_x, \kappa_t) \hookrightarrow (\alpha_x - c, \beta_x, \kappa_t + c) \tag{6}$$

produce the same outcome, as (α_x,β_x,κ_t) (see Appendix A).

As noted by Pitacco (Pitacco et al. 2009) the choice of the constraints is subjective, up to a point. In the literature the most used pair of constraints is

$$\sum_{t=t_1}^{t_n} \kappa_t = 0, \sum_{x=x_1}^{x_m} \beta_x = 1 \tag{7}$$

The model is estimated using the LS method

$$L = \min \sum_{x=1}^{N} \sum_{t=1}^{T} (\log(\hat{m}_{x,t}) - \alpha_x - \beta_x \kappa_t)^2 \tag{8}$$

Setting $\frac{d}{d\alpha_x}L = 0$ produces :

$$\sum_{t=t_1}^{t_n} \log(\hat{m}_{x,t}) = T\alpha_x + \beta_x \sum_{t=t_1}^{t_n} \kappa_t \tag{9}$$

and taking into account the constraint (6) $\sum_{t=t_1}^{t_n} \kappa_t = 0$, we get

$$\hat{\alpha}_x = \frac{1}{T} \sum_{t=1}^{T} \log(\hat{m}_{x,t}), \tag{10}$$

thus obtaining a general shape of the mortality curve. The parameters $\hat{\beta_x}$ and $\hat{\kappa_t}$ through SVD by introducing the $N \times T$ matrix

$$Z := \log(\hat{m}_{x,t}) - \hat{\alpha_x} \tag{11}$$

The newly introduced matrix can be decomposed to the matrices U, with dimensions $N \times N$, Σ, with dimensions $N \times T$, and V^T, with dimensions $T \times T$, which is the transpose of V.

$$Z = U\Sigma V^T \tag{12}$$

Let v_1 the eigenvector of the largest eigenvalue of V and u_1 the corresponding eigenvector of U. As seen in Pitacco (2009) the best approximation of Z in the LS method is

$$Z \approx \sqrt{\lambda_1} v_1 u_1^T, \tag{13}$$

where:

$$\hat{\beta} = \frac{v_1}{\sum_{j=1}^{N} v_{1,j}} \tag{14}$$

and

$$\hat{\kappa} = \sqrt{\lambda_1}(\sum_{j=1}^{N} v_{1,j}) u_1, \tag{15}$$

which satisfy the constraints imposed by (7).

First, from Figure 6 we can observe that the parameters of the LC model experience similar trends for males and females. α_x have a relatively high starting point and follow a steep downwards trend until approximately the age of 10. After this age, the age-specific pattern of mortality undergoes a linear evolution, with a small spike in the age of 20. Assuming the other parameters of the model remain constant, a higher α_x leads to a higher central mortality rate for each age group.β_x appear rather volatile in the young ages for both males and females. The latter exhibit a decrease from the age of 10 up until 60, when they display an upward trend up to the age of 75. Whereas, males display this upward trend at the age of 40 up until 60 with smaller steepness. κ_t experiences a steady downward decreasing trend as the years advance, with females showing lower values. This relates to the fact that going backwards in time the mortality levels boasted a higher level than the recent years. If the other parameters are kept constant, a lower value of κ_t will yield a decrease in the central mortality rate as the years pass.

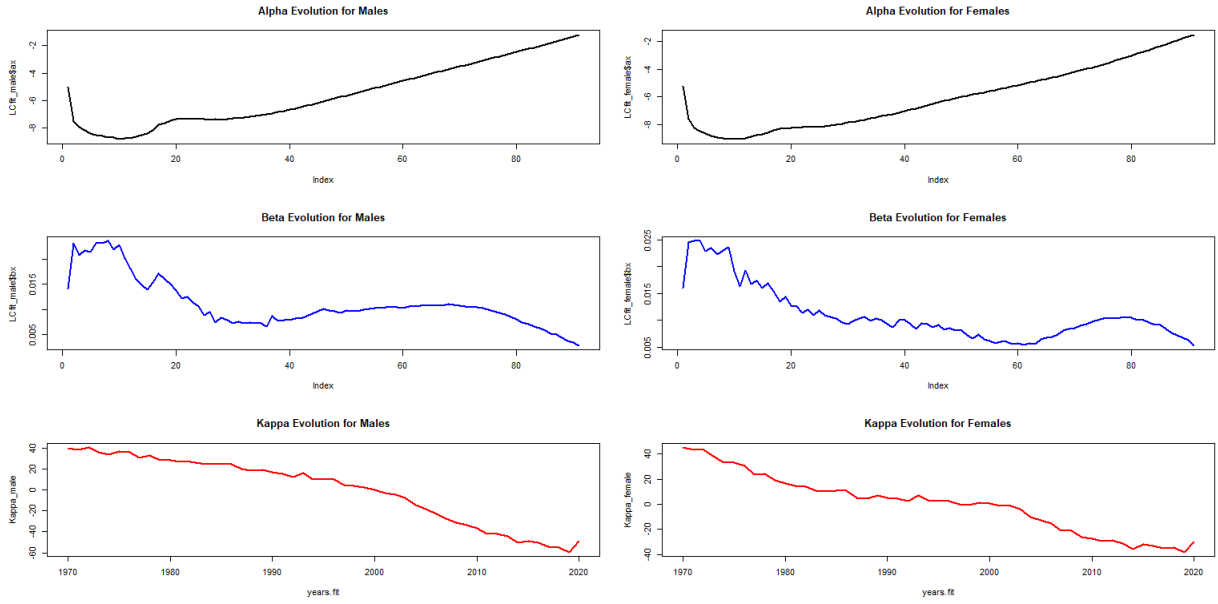

Figure 6: Parameters of LC model for Dutch male and female population with ages 0-90 for the period 1970-2020

5.2 Poisson log-bilinear model

5.2.1 Model Description

In 2002 Brouhns et.al (Brouhns, Denuit, and Vermunt 2002) developed a new method for constructing projected life tables using a Poisson regression approach. Brouhns et. al introduced the Poisson log-linear model as better and more intuitively accepted alternative. Originally, this model is implemented separately for each gender using data of age-specific death rates from Belgium. The assumption that errors are homoscedastic, implying that error terms are normally distributed for inference, is a significant point of criticism against the Lee-Carter approach, as it is considered unrealistic. It is argued that the variability of the logarithm of the observed force of mortality increases at older ages because of the significantly smaller number of deaths that occur at these ages. Therefore, it is considered that

$$D_{x,t} \sim \text{Poisson}(E_{x,t}\mu_{x,t}) \tag{16}$$

with $\mu_{x,t} = e^{(\alpha_x+\beta_x\kappa_t)}$, where $E_{x,t}$ is the exposure to risk, the number of person years from which the $D_{x,t}$ realized. The meaning of the α_x, β_x and κ_t parameters remains the same as the original Lee-Carter model.

5.2.2 Estimating the parameters

The term $\beta_x\kappa_t$ causes the force of mortality to behave log-binearly, thus rendering the use of LS inappropriate. Therefore, the definition of the parameters is conducted by maximizing the log-likelihood based on the Poisson distributional assumption, as given by:

$$L(\alpha,\beta,\kappa) = \sum_{x,t} D_{x,t}(\alpha_x + \beta_x\kappa_t) - E_{x,t}e^{\alpha_x+\beta_x\kappa_t} + c, \tag{17}$$

where c is a constant equal to -$\sum_x \sum_t D_{x,t}\log(E_{x,t}) + \log(D_{x,t})!$ (see Appendix A for derivations).

In order to solve the likelihood equations Newton's method is applied. The model poses three sets of parameters, namely $\alpha_x, \beta_x, \kappa_t$, which will be estimated by θ^ν following this iterative procedure:

$$\hat{\theta}^{(\nu+1)} = \hat{\theta}^{(\nu)} - \frac{L^\nu/d\theta}{d^2L^\nu/d\theta^2}, \tag{18}$$

where $L^{(\nu)}$=$L^{(\nu)}(\hat{\theta}(\nu))$.

In order to start the iterative scheme, random values need to be assigned to $\alpha_x, \beta_x, \kappa_t$. In the paper by Brouhns et. al (2002) $\alpha_x = 0, \beta_x = 0, \kappa_t = 1$, the set of parameters updates as follows:

$$\hat{\alpha_x}^{(\nu+1)} = \hat{\alpha_x}^{(\nu)} - \frac{\sum_t (D_{x,t} - \hat{D}_{x,t}\,\nu)}{-\sum_t \hat{D}_{x,t}^{\nu}}, \hat{\beta_x}^{(\nu+1)} = \hat{\beta_x}^{(\nu)}, \hat{\kappa_t}^{(\nu+1)} = \hat{\kappa_x}^{(\nu)},$$

$$\hat{\kappa_t}^{(\nu+2)} = \hat{\kappa}^{(\nu+1)} - \frac{\sum_x (D_{x,t} - \hat{D}_{x,t}^{(\nu+1)})\hat{\beta}_x^{(\nu+1)}}{-\sum_x \hat{D}_{x,t}^{\nu} (\beta_x^{(\nu+1)})^2}, \hat{\alpha_x}^{(\nu+2)} = \hat{\alpha_x}^{(\nu+1)}, \hat{\beta_x}^{(\nu+2)} = \hat{\beta_x}^{(\nu+1)},$$

$$\hat{\beta_x}^{(\nu+3)} = \hat{\beta_x}^{(\nu+2)} - \frac{\sum_t (D_{x,t} - \hat{D}_{x,t}^{(\nu+2)})\hat{\kappa}_t^{(\nu+2)}}{-\sum_t \hat{D}_{x,t}^{(\nu+2)} (\kappa_t^{(\nu+3)})^2}, \hat{\alpha_x}^{(\nu+3)} = \hat{\alpha_x}^{(\nu+2)}, \hat{\kappa_t}^{(\nu+3)} = \hat{\kappa_t}^{(\nu+2)}, \tag{19}$$

where $\hat{D}_{x,t}^{(\nu)} = E_{x,t}\, e^{\alpha_x + \beta_x \kappa_t}$, the estimated number of iterations of step ν. The criterion to stop the algorithm is a very small increase of the log-likelihood function (i.e. as recommended in the paper 10^{-10})[1].

In order to avoid the identification problems constraints need to be imposed, as in the Lee-Carter model. After updating the κ_t parameters, the constraint $\sum_t \hat{\kappa}_t = 0$ is imposed. After updating the β_x parameters, a scaling constraint has to be imposed. To obtain the same parameterization as in the Lee-Carter approach,$\sum_x \hat{\beta}_x = 1$, the estimates for β_x are divided by $\sum_x \hat{\beta}_x$ and the estimates for κ_t are multiplied by the same number.

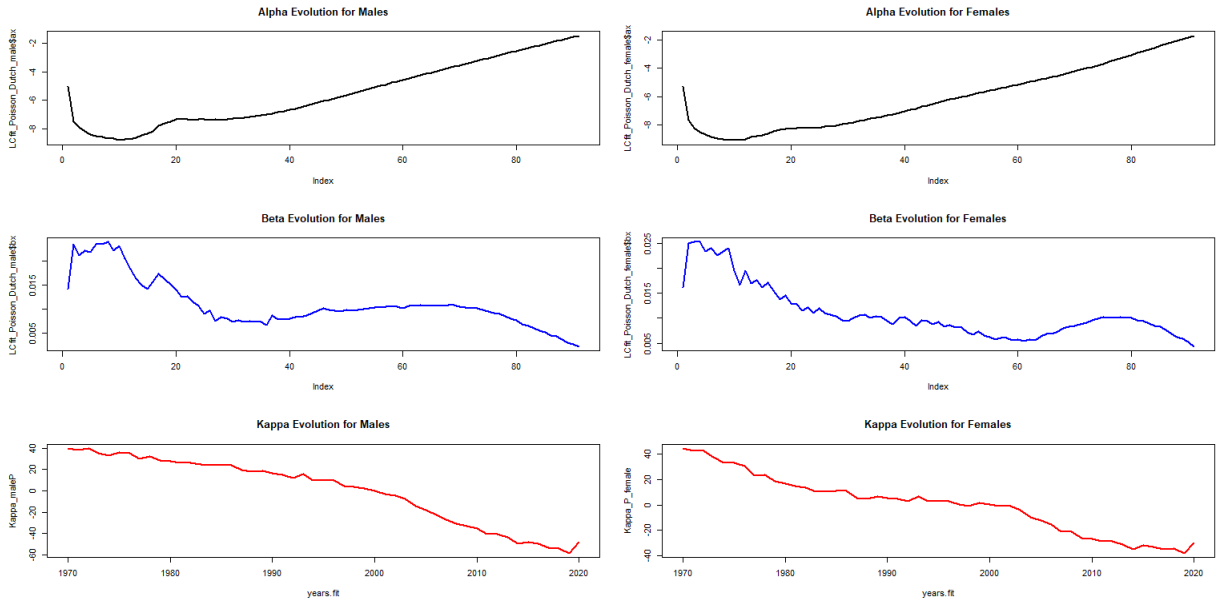

Figure 7: Parameters of LC model in the Poisson Setting for Dutch male population with ages 0-90 for the period 1970-2021.

From Figure 7 we can deduct that the parameter evolution in the LC Poisson setting resembles the evolution of the original Lee-Carter. Similarly, α_x follow an upward trend with a higher spike for males in the age of 20 than their female counterparts. Females, also, display lower values for β_x and κ_t as described in the figures of the original LC model.

[1]This can be perceived as that the algorithm stops when there is a very small increase in the log-likelihood and subsequently the improvement of the estimates of the parameters is unimportant.

5.3 Li-Lee model

5.3.1 Model Description

Contrary to the classical Lee-Carter model, Lee and Li (2005) recommended drawing on the international context in order to improve individual country's mortality projections. The Li-Lee model (LL), an extension to the classical LC model, falls into the coherent mortality models category. In such models, a general trend across the members of the group is presented and in order to extract country specific mortality information, this country's deviance from the shared trend is calculated.

Similar countries' data are merged in order to create a super-population. In terms of mortality, the Gross Domestic Product (GDP) is considered the primary measure of similarity along the corresponding literature, as there exists a positive correlation of the GDP and life expectancy. A multi-populational model forecasting mortality rates for an individual population has the benefit of integrating more information points, allowing for the identification of shared trends across a broader range of populations, thus avoiding avoid diverging projected mortality rates in similar countries, which has been deemed as inaccurate.

$$\log(m_{x,t,i}) = \alpha_{x,i} + B_{x,i}K_{t,i} + \beta_{x,i}\kappa_{t,i} + \epsilon_{x,t,i}, \tag{20}$$

where i refers to a specific country in the group. The terms used in formula (19) have the same function as in the LC model. However, it can be seen that an additional term has been included. B_xK_t is the common factor in the model and accounts for the changes in mortality for the whole group of countries. $\beta_{x,i}\kappa_{t,i}$ are country specific and explain the short term fluctuations for the ith population and allow short term divergence between the group members, whereas B_xK_t ensures the long term convergence.

5.3.2 Estimating the parameters

The ordinary LC approach is applied for the entire population in order obtain the common values for B_x and K_t. Continuing, K_t is adjusted to fit the group's average life expectancy.

$\alpha_{x,i}$ are estimated independently for each country i, since they do not account for long term divergence between the groups. In order to obtain estimates for $\alpha_{x,i}$, the OLS method can be applied :

$$\min \sum_{t=0}^{T} [(\log(m_{x,t,i}) - \alpha_{x,i} - B_xK_t]^2 \tag{21}$$

Due to the constraint $\sum_t K_t = 0$,

$$\alpha_{x,i} = \frac{\sum_{t=0}^{T} \log(m_{x,t,i})}{T+1}, \tag{22}$$

which yields the same result as when the LC is applied to the i^{th} country separately.

Following the LC methodology, SVD is applied to the residual matrix of the common factor model, $[\log(m_{x,t,i}) - \alpha_{x,i} + B_xK_t]$. The first order vectors $\beta_{x,i}$ and $\kappa_{t,i}$ are derived, allowing us to obtain the specific factor of ith group member, which is denoted as $\beta_{x,i}\kappa_{t,i}$ and thus resulting in the model described by (19).

$\kappa_{t,i}$ is forecasted using a first-order autoregressive model AR(1) :

$$\kappa_{t,i} = c_{0,i} + c_{1,i}\kappa_{t-1,i} + \sigma_i\epsilon_i, \tag{23}$$

with $\epsilon_{i,t} \sim N(0,1)$. It is worth mentioning that $\kappa_{t,i}$ can, also, be forecasted by employing a random walk without drift model.

It is evident from Figures 8 and 29 (see Appendix B that the parameters in the LL model experience a similar evolution for males and females. For males, the European common term B_x follows a downward trend until

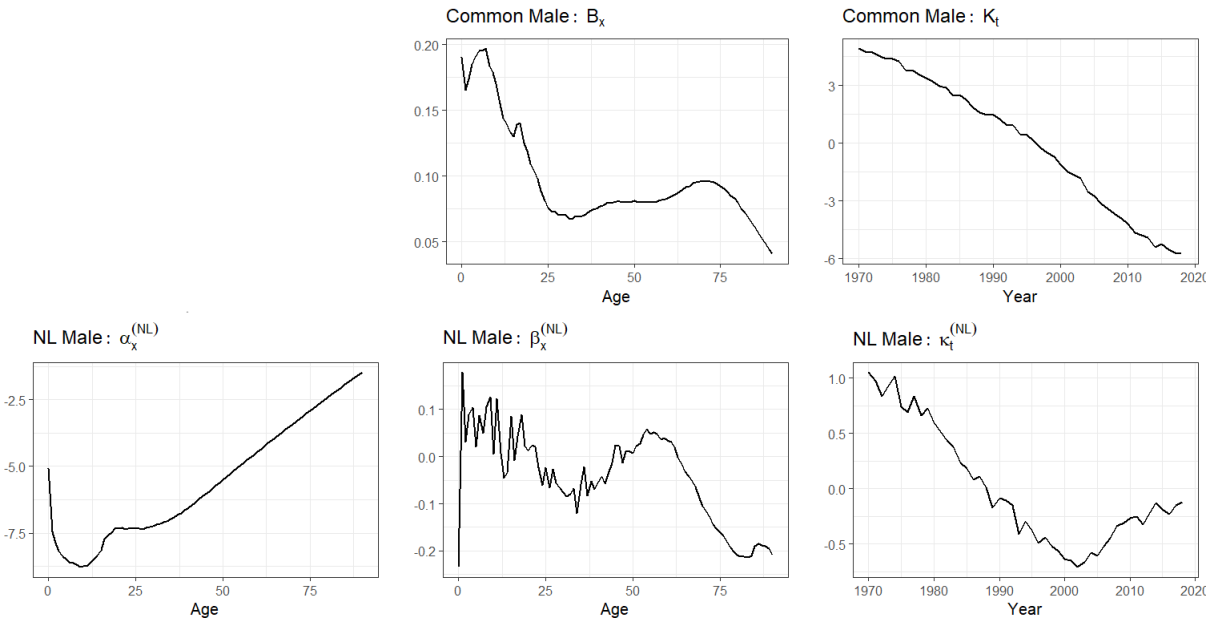

Figure 8: Parameters of LL model for Dutch male population with ages 0-89 for the period 1970-2019.

the age of 25 and then it increases until 70 and then drops again. Whereas for females there is less variation, as a decrease is depicted until 55, with a small increase up to the age of 75 and the again a drop is shown. The period indices K_t and κ_t can be described as having a downwards trends for both sexes, with more variation being noted on the country specific parameter. It is worth noting that κ_t decreased up to 2000 and then experienced an increase. The country specific α_x followed an evolution similar to the previous models. For the country specific β_x great variation can be observed. β_x for males showed a steep decrease after the age of 55, whereas for females it plateaued after the age of 40.

5.4 AG model

5.4.1 Model Description

In the Netherlands, AG (Actuarieel Genootschap) is the organization responsible for producing the future mortality projections of the Dutch society. The model currently utilized by AG is a type of Li-Lee model. Following the Li-Lee approach, the Dutch mortality data-set is merged with the corresponding information from other similar countries, whereas males and females are modelled jointly. Here, the value of GDP is ,also, the primary measure of similarity. Countries with a higher than average GDP, as the Netherlands, are grouped together to create a super-population. The selection of these countries, as noted in AG2022 (AG 2022), includes: Netherlands, Belgium, Denmark, Germany, Finland, France, Ireland, Iceland, Luxembourg, Norway, Austria, the UK, Sweden and Switzerland. The incorporation of additional information allows the model to be more stable and avoid the strong correlation to the historic Dutch deviations from the trend (Antonio et al. 2017) and the fact that there is a proven positive correlation between ageing and prosperity ensures that the results will not be skewed in a wrong direction.

AG models the logarithm of the force of mortality for the Netherlands, as follows :

$$\log(m_{x,t}) = \log(m_{x,t}^{EU}) + \log(m_{x,t}^{NL}), \tag{24}$$

where:

$$\log(m_{x,t}^{EU}) = A_x + B_x K_t \tag{25}$$

$$\log(m_{x,t}^{NL}) = \alpha_x + \beta_x \kappa_t \tag{26}$$

The model in use employs a similar method to the Li-Lee model (2005), following an approach that can be characterized as a double Lee-Carter. The first step involves capturing the European trend, where 25 refers to a LC model for the European progression of mortality driven by ($m_{x,t}^{EU}$). Followed by fitting the model to the Dutch data for each gender, with 26 being a LC model concerning the Dutch deviation from the common trend (specified by $m_{x,t}^{NL}$).

A difference from the original Li-Lee model should be noted. The AG model incorporates an additional common parameter A_x, as can be seen in 20 25, which is an age specific factor driven by information of the whole group.

5.4.2 Estimating the parameters

The parameters in the AG model are estimated using MLE, as opposed to the SVD approach employed in the Li-Lee model. The calibration methodology is applied independently on male and female data. A Poisson distribution, as in Brouhns et al. (2002), is assumed for the number of deaths $D_{x,t}$, with mean $E_{x,t} \cdot \mu_{x,t}$ and $E_{x,t}$ exposure to risk. A_x, B_x, K_t are calibrated on the aggregated European data in the first step, followed by the estimation of the country specific factors (in this case the Netherlands) $\alpha_x, \beta_x, \kappa_t$ using country-specific data in the second step (ibid.). In detail (AG 2020) (AG 2022):

1. The exposures $E_{x,t}^{EU}$ and the observed deaths $D_{x,t}^{EU}$ are the sum of all exposures and deaths from the super-population of the prosperous Western countries (including the Netherlands). The parameters A_x, B_x, K_t are estimated such that the Poisson likelihood is maximized :

$$\max_{A_x, B_x, K_t} \prod_x \prod_t \frac{(E_{x,t}^{EU} m_{x,t}^{EU})^{D_{x,t}^{EU}} e^{(-E_{x,t}^{EU} m_{x,t}^{EU})}}{D_{x,t}^{EU}!}, \tag{27}$$

   with $m_{x,t}^{EU} = e^{A_x + B_x K_t}$. In order to ensure identification of the estimated parameters, the following constraints are imposed :

$$\sum_{t}^{t_n} K_t = 0, \sum_{x}^{x_m} B_x = 1 \tag{28}$$

2. Using the estimations obtained in the previous step $\hat{A}_x, \hat{B}_x, \hat{K}_t$, the MLE method is applied to the Dutch mortality data-set in order to calibrate the parameters $\alpha_x, \beta_x, \kappa_t$:

$$\max_{\alpha_x, \beta_x, \kappa_t} \prod_{x} \prod_{t} \frac{(E_{x,t}^{NL} m_{x,t}^{NL})^{D_{x,t}^{NL}} e^{(-E_{x,t}^{NL} m_{x,t}^{NL})}}{D_{x,t}^{NL}!}, \tag{29}$$

where: $m_{x,t}^{NL} = \hat{m}_{x,t}^{EU} = e^{A_x, + B_x K_t} \cdot e^{\alpha_x + \beta_x \kappa_t}$, with $\hat{m}_{x,t}^{EU} = e^{\hat{A}_x + \hat{B}_x \hat{K}_t}$. As the previous step, normalization is applied :

$$\sum_{t=t_1}^{t_n} \kappa_t = 0, \sum_{x=x_1}^{x_m} \beta_x = 1 \tag{30}$$

3. In order to yield predictions for the future mortality, the time effect index in Europe K_t is modelled as a random walk with drift, whereas the Dutch deviation κ_t is modelled by a fist order autoregressive AR(1) model, producing the following equations :

$$K_t = K_{t-1} + \theta + \epsilon_t \tag{31}$$

$$\kappa_t = \alpha \kappa_{t-1} + c + \delta_t, \tag{32}$$

where θ is the estimated drift of the time index in Europe, c, α are the estimated constant terms and the estimated AR(1) term of the time effects in the Dutch deviation and ϵ_t, δ_t are the error terms.

From Figures 9 and 10 the most evident finding that can be inferred is the contrasting evolution between the super-population (European countries) parameters and the country-specific (Netherlands) parameters. β_x^{EU} and κ_t^{EU} experience a similar pattern with the common factors B_x and K_t of the Li-Lee model, whereas the evolution of α_x^{EU} resembles the evolution of α_x^{NL} in the same model. Moreover, it is important to note that the parameters are not significantly different between genders. α_x^{EU} appears steadily increasing in age while experiencing the hump in the age of 20 as the models before, whereas α_x^{NL} undergoes a lot more variation with a significant drop for ages 10-20 and an increase up to the age of 90. β_x^{EU} decreases continuously as the ages become bigger, whereas β_x^{NL} encounter noticeable variation while following an increasing trend. κ_t^{EU} is decreasing in years in contrast to its country-specific counterpart κ_t^{NL}, which experiences a decreasing tendency after 2000 for males and remains at the same level with fluctuations for females after the same time point.

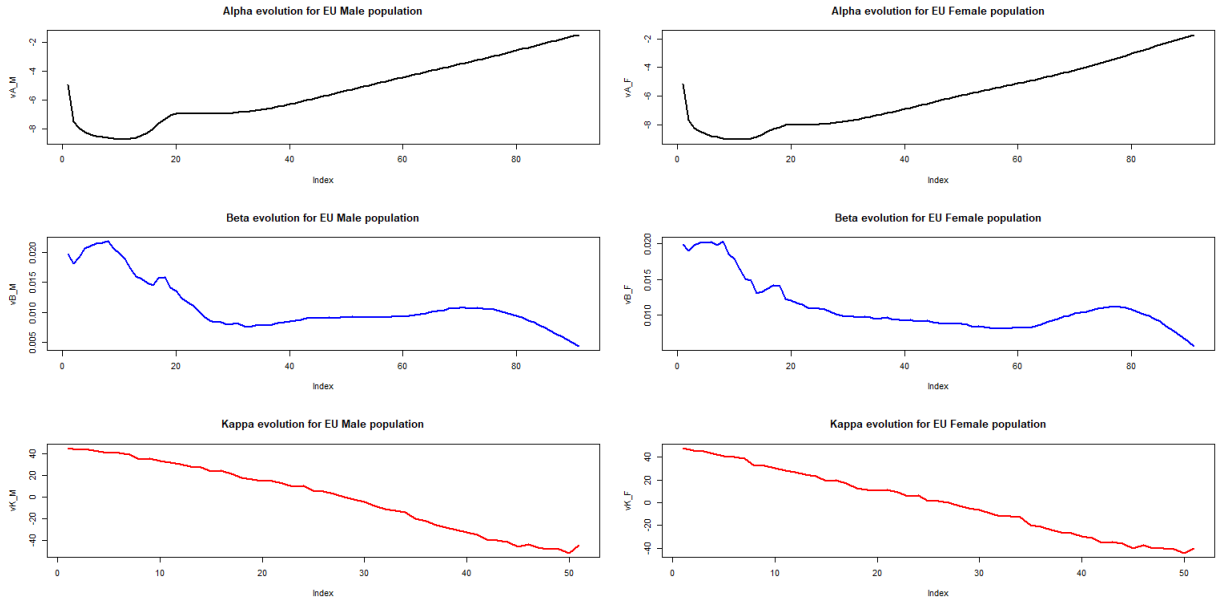

Figure 9: Parameters of AG model for the selected European countries for male and female population with ages 0-90 for the period 1970-2019.

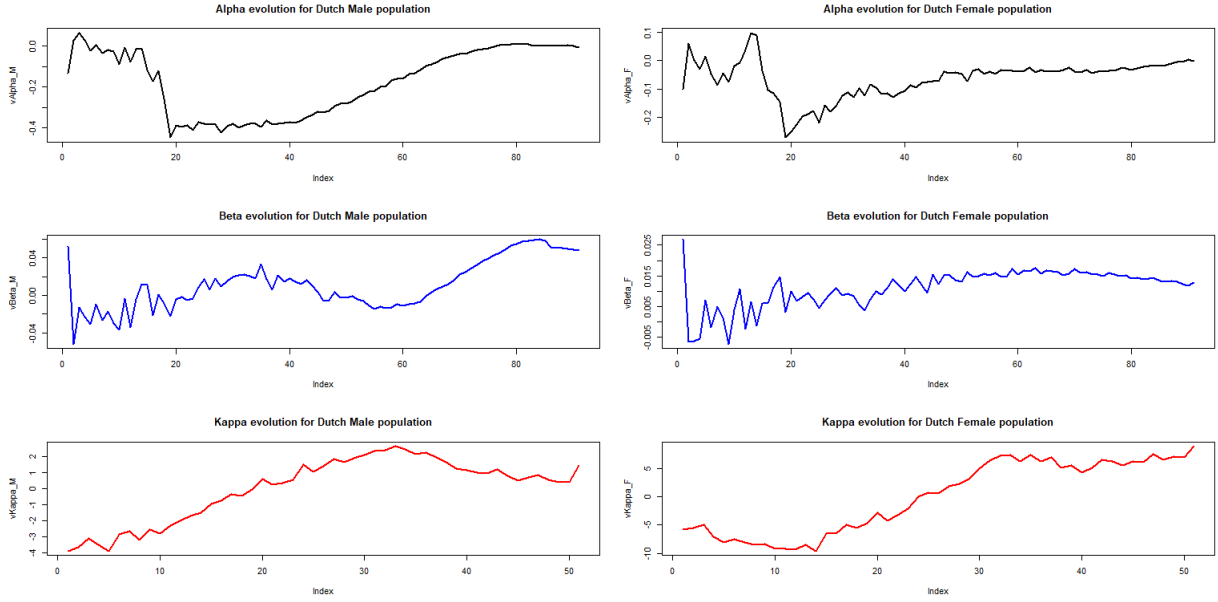

Figure 10: Parameters of AG model for Dutch population for male and female population with ages 0-90 for the period 1970-2019.

5.5 Renshaw Haberman model

5.5.1 Model Description

Willets (Willets 2004) observed that individuals born in the U.K. between 1925 and 1945 have witnessed faster improvements in mortality rates compared to the generations born before or after this period. (Hatzopoulos and Haberman 2015), with this phenomenon being widely considered to be partially due to the varying smoking habits of different generations. This phenomenon is referred to as cohort effect.

In the above models it can be seen that the cohort effect has been neglected. However, as the financial implications of mortality risk have become more apparent, there has been a significant rise in interest regarding the cohort aspect of mortality. This concept links the biological effects of aging to the effects of current factors and the influence of an individual's past history on mortality, as described by Hobcraft et al. (Hobcraft, Menken, and Preston 1982). However, it is recognized that this breakdown is challenging because the equation $cohort = period - age$ complicates the distinct separation of interdependent changes across the three dimensions (Villegas Ramirez 2015).

Therefore, Renshaw and Haberman (2006) proposed an extension of the original LC model which incorporates the cohort effects. The cohort effect captures the influence of the year of birth on the mortality rates of different generations. The model was proposed as a way to improve the fit and the forecasting performance of the Lee-Carter model (ibid.), especially for older ages where the cohort effect is more pronounced. The aforementioned cohort effect is incorporated in the model as follows:

$$\log(m_{x,t}) = \alpha_x + \beta_x^{(1)}\kappa_t + \beta_x^{(0)}\boldsymbol{\iota_{t-x}}, \tag{33}$$

where the reduction factor is:

$$RF_{x,t} = e^{(\beta_x^{(1)}\kappa_t + \beta_x^{(0)}\iota_{t-x})}, \tag{34}$$

which contains both the age-specific (κ_t) and cohort (ι_{t-x}) effects.

The parameters $\alpha_x, \beta_x^{(1)}, \kappa_t$ have the same interpretation as in the original LC model, while the newly added term "ι_{t-x} controls the specific features of mortality for individuals from the same cohort with $\beta_x^{(0)}$ modulating its effect across the age range" (Hunt and A. Villegas 2015).

5.5.2 Estimating the parameters

Similarly to the base model Lee-Carter, the RH model faces identification issues too, since the following transformations of the parameters leave 33 unchanged:

$$(\overline{\alpha}_x, \overline{\beta}_x^{(1)}, \overline{\kappa}_t, \overline{\beta}_x^{(0)}, \overline{\iota}_y) \hookrightarrow (\alpha_x, a\beta_x^{(1)}, \frac{1}{a}\kappa_t, \beta_x^{(0)}, \iota_y) \tag{35}$$

$$(\overline{\alpha}_x, \overline{\beta}_x^{(1)}, \overline{\kappa}_t, \overline{\beta}_x^{(0)}, \overline{\iota}_y) \hookrightarrow (\alpha_x, \beta_x^{(1)}, \kappa_t, b\beta_x^{(0)}, \frac{1}{b}\iota_y) \tag{36}$$

$$(\overline{\alpha}_x, \overline{\beta}_x^{(1)}, \overline{\kappa}_t, \overline{\beta}_x^{(0)}, \overline{\iota}_y) \hookrightarrow (\alpha_x - c\beta_x^{(1)}, \beta_x^{(1)}, \kappa_t + c, \beta_x^{(0)}, \iota_y) \tag{37}$$

$$(\overline{\alpha}_x, \overline{\beta}_x^{(1)}, \overline{\kappa}_t, \overline{\beta}_x^{(0)}, \overline{\iota}_y) \hookrightarrow (\alpha_x - d\beta_x^{(0)}, \beta_x^{(1)}, \kappa_t, \beta_x^{(0)}, \iota_y + d) \tag{38}$$

In order to ensure a unique set of parameter estimates, the following constraints were imposed (ibid.):

$$\sum_x \beta_x^{(1)} = 1 \tag{39}$$

$$\sum_x \beta_x^{(0)} = 1 \tag{40}$$

$$\sum_{t} \kappa_{t_1} = 0 \tag{41}$$

In their original paper (Renshaw and Haberman 2006) Renshaw and Haberman employed two-stage fitting procedure to fit the model to data. In the aforementioned procedure, "first the main age effects (α_x) are set to be $(\alpha_x) = \frac{1}{n}\sum_t \log(\frac{D_{x,t}}{E_{x,t}})$ and then the other parameters are found sing an iterative approach which maximises the log-likelihood, without updating the term (α_x)" (Hunt and A. Villegas 2015).

However, this approach received criticism regarding the speed of convergence to an optimum result and the lack of robustness to changes in data, as highlighted by (A. Cairns et al. 2007b) and (Institute and Actuaries 2007). Cairns et. al. (2009) proposed to fit all the parameters from 33 simultaneously by employing a Poisson likelihood maximization approach. The understanding that extra constraints were necessary to ensure unique identification prompted Cairns et al. (2009) to implement the following additional constraints:

$$\sum_{t=t_1}^{t_n} \kappa_t = 0 \tag{42}$$

$$\sum_{t=t_1}^{t_n} \sum_{x=x_1}^{x_k} \iota_{t-x} = 0 \tag{43}$$

In order to produce the parameter estimates in this thesis the algorithm[2] presented in Algorithm 1 is employed. This approach helps to solve the aforementioned convergence and robustness problems. The function follows the constraints imposed by (Hunt and A. Villegas 2015) who assume a variation of (43) and impose:

$$\sum_{y=t_1-x_k}^{t_n-x_1} \iota_y = 0, \tag{44}$$

The parameter estimates are derived by maximising the log likelihood:

$$L(D_{x,t}, \hat{D}_{x,t}) = \sum_x \sum_t w_{x,t} D_{x,t} \log \hat{D}_{x,t} - \hat{D}_{x,t} - \log \hat{D}_{x,t}!, \tag{45}$$

where $\hat{D}_{x,t} = e_{x,t} e^{\alpha_x + \beta_x^{(1)} \kappa_t + \beta_x^{(0)} \iota_{t-x}}$ and $w_{x,t}$ are $0-1$ weights for empty or omitted data cells.

[2] the function *fit.rh()* from the package *StMoMo* in R is used

Algorithm 1 Algorithm 1 Maximum likelihood parameter estimation procedure for RH model (Hunt and A. Villegas 2015)

1. **Set** initial values for $\hat{\alpha}_x$,$\hat{\beta}_x^{(1)}$,$\hat{\kappa}_t$,$\hat{\iota}_y$; **compute** $\hat{D}_{x,t}$; and **compute** $L(d_{x,t}, \hat{D}_{x,t})$.

2. **Update** $\hat{\alpha}_x$ and **compute** $\hat{D}_{x,t}$.

3. **Update** $\hat{\kappa}_t$; **set** $c := \frac{1}{n}\sum_t \hat{\kappa}_t, \hat{\kappa}_t := \hat{\kappa}_t - c, \hat{\alpha}_x := \hat{\alpha}_x + c\hat{\beta}_x^{(1)}$ to ensure $\sum_t \kappa_t^{(1)} = 0$; and **compute** $\hat{D}_{x,t}$.

4. **Update** $\hat{\beta_x}^{(1)}$; **set** $\alpha := \frac{1}{\sum_x \hat{\beta_x}^{(1)}}, \hat{\beta_x}^{(1)} := \alpha\hat{\beta_x}^{(1)}, \hat{\kappa}_t := \frac{1}{\alpha}\hat{\kappa}_t$ to ensure $\sum_x \beta_x^{(1)} = 1$; and **compute** $\hat{D}_{x,t}$.

5. **Update** $\hat{\iota}_y$; **set** $D := \frac{1}{n+k-1}\sum_y \hat{\iota}_y, \hat{\iota}_y := \hat{\iota}_y - d, \hat{\alpha}_x := \hat{\alpha}_x + D\hat{\beta}_x^{(0)}$ to ensure $\sum_y \hat{\iota}_y = 0$; and **compute** $\hat{D}_{x,t}$.

6. **Update** $\hat{\beta}_x^{(0)}$; **set** $b := \frac{1}{\sum_x \hat{\beta}_x^{(0)}}, \hat{\beta}_x^{(0)} := b\hat{\beta}_x^{(0)}, \hat{\iota}_y := \frac{1}{b}\hat{\iota}_y$ to ensure $\sum_x \hat{\beta}_x^{(0)} = 1$; and **compute** $\hat{D}_{x,t}$.

7. **If** the constraint $\sum_{y=t_1-x_k}^{t_n-x_1}(y-\overline{y})\iota_y$ is imposed using the transformation $(\overline{\alpha}_x, \overline{\beta}_x^{(1)}, \overline{\kappa}_t, \overline{\beta}_x^{(0)}, \overline{\iota}_y) \hookrightarrow \{\alpha_x + e\beta_x^{(0)}(x-\overline{x}), \frac{K}{K-e}\beta_x^{(1)} - \frac{e}{K-e}\beta_x^{(0)}, \frac{K-e}{K}\kappa_t, \beta_x^{(0)}, \iota_y + e(y-\overline{y})\}$ **Set** $K := \sum_t(t-\overline{t})\hat{\kappa}_t / \sum_t(t-\overline{t})^2$, $e := -\sum_y(y-\overline{y})\hat{\iota}_y / \sum_y(y-\overline{y})^2$, $\hat{\alpha}_x := \hat{\alpha}_x + e\hat{\beta}_x^{(0)}(x-\overline{x})$,$\hat{\beta}_x^{(1)} := \frac{K}{K-e}\hat{\beta}_x^{(1)} - \frac{e}{K-e}\hat{\beta}_x^{(0)}$,$\hat{\kappa}_t := \frac{K-e}{K}\hat{\kappa}_t$, $\hat{\iota}_y := \hat{\iota}_y + e(y-\overline{y})$ to ensure $\sum_y(y-\overline{y})\hat{\iota}_y = 0$; and **compute** $\hat{D}_{x,t}$.

8. **Compute** $L(D_{x,t}, \hat{D}_{x,t})$.

9. **If** $L(D_{x,t}, \hat{D}_{x,t})$ has not converged **go to 2**.

10. **Return** $\hat{\alpha}_x$,$\hat{\beta}_x^{(1)}$,$\hat{\kappa}_t$,$\hat{\iota}_y$.

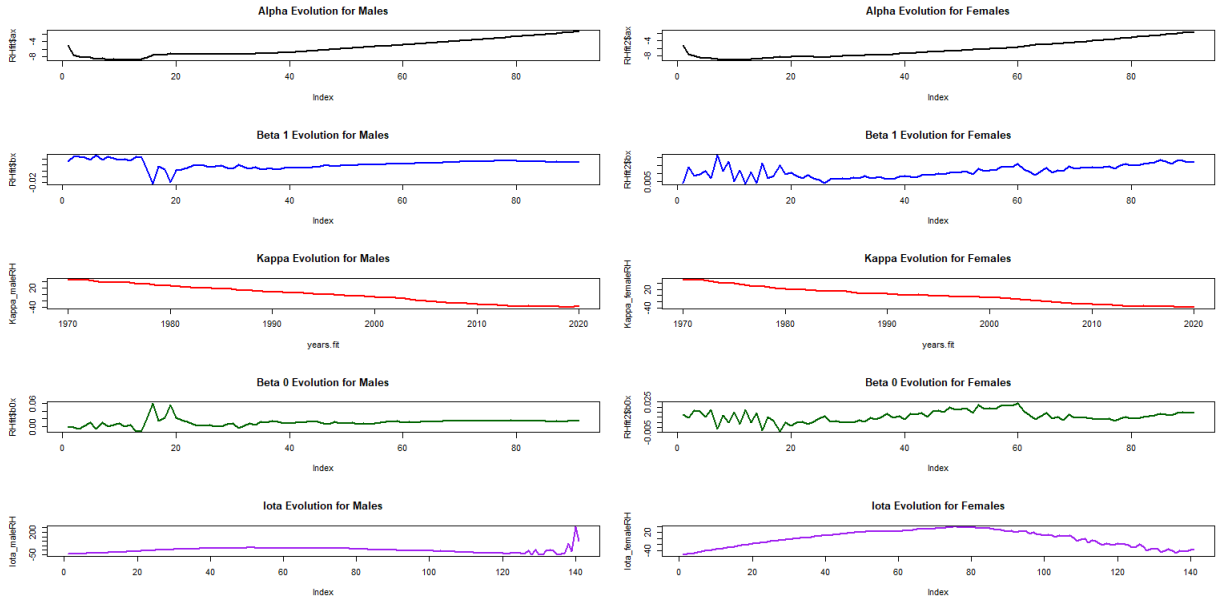

Figure 11: Parameters of RH model for Dutch male population with ages 0-90 for the period 1970-2019.

Figure 11 depicts the α_x evolution is similar in males and females, with males once again having a higher spike in the age of 20, and also follows an increasing trend as shown in the previous models. The period index κ_t again shows a decreasing evolution, which translates to a general drop of mortality levels. In β_x^1 we can observe the first differences between the models. Although volatile, both male and female experience an increasing trend as opposed to the Lee-Carter model, which can be seen as the increase of sensitivity to the term κ_t, as people get older. The β_x^0 parameter follows a decreasing evolution for males. It is volatile between the ages 0-20 and plateaus after the age of 35. Whereas for their female counterparts, β_x^0 is very volatile and experiences an increasing term for the largest part. Finally, the parameter ι_{t-x} (displayed as γ in the plot) shows an upward trend up until 1950 and then decreases for both males and females. This is translated as that the mortality levels for the cohorts included in 1880-1950 were increasing and mortality levels for individuals born after 1950 dropped.

6 Data

The mortality data in this thesis is obtained from the HMD website (Human Mortality Database). The HMD project has stringent data quality standards and is only applicable to countries with reliable population data. The project took approximately two years to finish and is currently regarded as one of the most frequently utilized and referenced data sources in the fields of demography and mortality.

The complete data series include the six following types of data for different countries ((ibid.)) :

- **Births**: Births are registered on an annual basis and categorized by gender for various populations during different time frames.
- **Deaths**: Death counts are collected at the finest level of detail available. If raw data are aggregated, uniform methods are used to estimate death counts by completed age (i.e., age-last-birthday at time of death), calendar year of death, and calendar year of birth.
- **Population size on January** 1^{st}: Annual estimates of population size on January 1^{st}.
- **Exposure-to-risk**: Estimates of the population exposed to the risk of death during some age-time interval are based on annual (January 1^{st}) population estimates, with a small correction that reflects the timing of deaths within the interval.
- **Death rates**: Death rates are always a ratio of the death count for a given age-time interval divided by an estimate of the exposure-to-risk in the same interval.
- **Life tables**: Probabilities of death are computed from death rates. These probabilities are used to construct life tables, which include life expectancy and other useful indicators of mortality and longevity.

In the cases of the Li-Lee and AG models data from multiple countries are employed. In order to produce enhanced results for the Dutch mortality projections, a super-population of countries is created. According to the AG website, the selection of countries that accompany the Netherlands is based on prosperity, which is measured with each country's GDP. This lies in the assumption that there exists a positive correlation between ageing and prosperity. The selected countries share an above average GDP per capita. Below the selection of countries and the corresponding available data can be seen:

List of Countries	
Country	Years
Netherlands	1850 - 2021
Belgium	1841 - 2022[3]
Denmark	1835 - 2022
Germany	1956 - 2020[4]
Finland	1878 - 2022
France	1816 - 2021
Ireland	1950 - 2020
Iceland	1838 - 2021
Luxembourg	1960 - 2022
Norway	1846 - 2022
Austria	1947 - 2019
U.K.	1922 - 2020
Sweden	1751 - 2022
Switzerland	1876 - 2022

Table 1: List of countries used in the AG selection and the corresponding availability of data

The data used runs from 1970 up until 2019 and the ages range from 0 up to 90 years old. The selection of years allows to establish a common ground for the countries and to ensure stability, as certain shocks (e.g. Spanish Influenza, World War II) are avoided, while the ages used help to steer clear of problems with exceptionally old ages (e.g. 100) with few data points which are extremely volatile.

Figure 12 depicts the distribution of mortality, for the year 2019, across the selected countries.

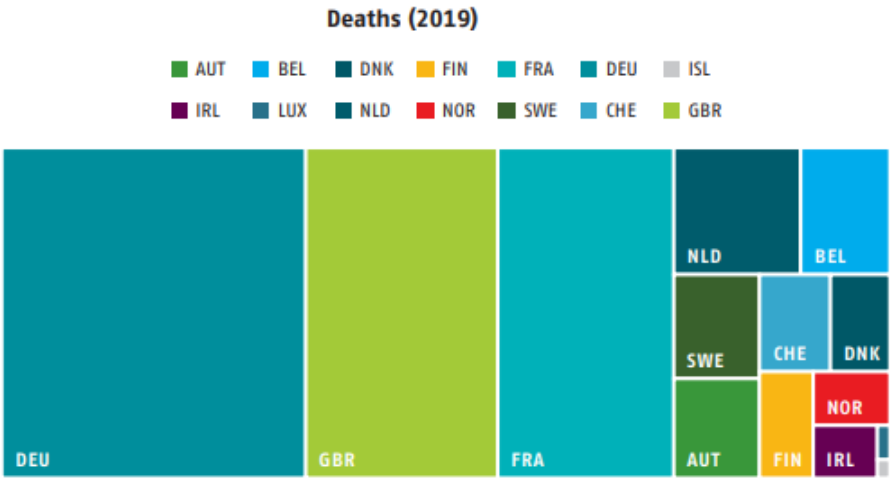

Figure 12: Spread of deaths (male and female) in 2019 by country Source: Projections Life Table (AG 2022)

[3]Gap in the HMD data series for years 1914-1918 in Belgium due to the lack of mortality statistics for this period.
[4]Data from West Germany used up to 1989.

7 Forecasting

After the development of a theoretical framework regarding a variety of mortality models and the analysis of their dynamics and mechanisms, space has been created in order to explore the models' performance in the field of forecasting.

7.1 Random Walk with drift

In the forecasting process the terms α_x and β_x remain constant, while κ_t evolves and thus extrapolation is required. It should be noted that, also, the cohort term $\boldsymbol{\iota_{t-x}}$ in the Renshaw-Haberman model can be extrapolated into the future, however in this thesis the review is focused on forecasting the time index κ_t.

Lee and Carter in 1992, after employing Box-Jenkins methods, concluded that modelling κ_t as a random walk with drift fits the data best. The time index is predicted to decline at a constant linear rate and is projected into the future using an AutoRegressive Integrated Moving Average (0,1,0) process and

An ARIMA(p,d,q) model is given by:

$$X_t = b_0 + b_1 X_{t-1} + b_2 X_{t-2} + ... + b_p X_{t-p} \epsilon_t + \phi_1 \epsilon_{t-1} + ... + \phi_q \epsilon_{t-q}, \tag{46}$$

where:

- **p**: The order of the autoregressive (AR) part, which means how many past values of the series are used to predict the current value.
- **d**: The order of differencing (I), which means how many times the series is differenced to make it stationary
- **q**: The order of the moving average (MA) part, which means how many past forecast errors are used to adjust the current prediction.

In the case of ARIMA(0,1,0) (Levendis 2018), which means employing differencing once (d=1):

$$X_t - X_{t-1} = b_0 + \epsilon_t, \tag{47}$$

where substituting $X_t = \kappa_t$, $X_{t-1} = \kappa_{t-1}$ and $b_0 = \theta$ yields 3 described in 5.1.1.

It is noteworthy to mention that, also, different values of p, d, q could be chosen for the ARIMA process to fit the data, however in this thesis it is opted to adhere to the original propositions of Lee and Carter for the LC and RH models. In Figure 13 the historical and projected evolution of κ_t for Dutch males and females in the Lee-Carter setting is displayed,[5] as well as for the Poisson setting and the Renshaw-Haberman model (see Appendix B Figures 30 and 31.

[5]In a fan chart graphs of observed past data and future predictions are combined. Predictions are displayed with ranges of possible values together with a line showing a central estimate or most likely value of future outcomes.(Wikipedia contributors 2022)

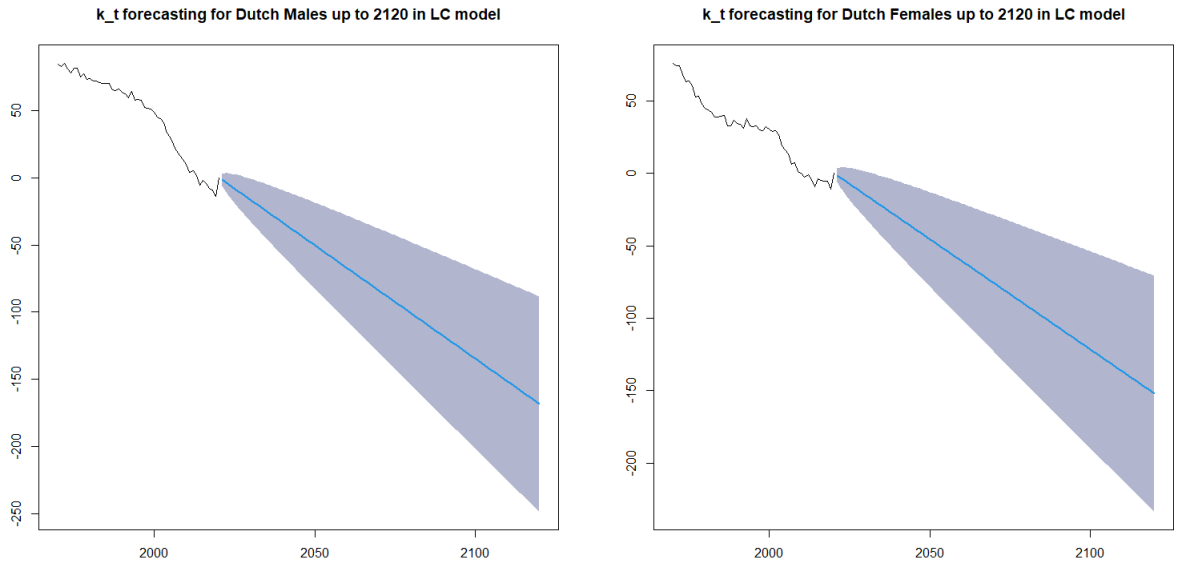

Figure 13: Evolution of κ_t in the LC model over 1970-2020 and forecasting 100 years into the future.

7.2 Cohort and Period Life Expectancy

Life expectancy refers to the expected duration of life for a population, estimated from the birth year, current age, sex, and other variables that influence mortality. A life table is employed in order to estimate life expectancy, which displays the likelihood of dying before the next birthday for each age group. Life tables can be classified into two categories: period and cohort.

A cohort life table estimates the lifespan of a population group that shares the same birth year (or a group of years), based on the observed and projected mortality rates for each age over their lifetime. For instance, the cohort life expectancy at age 65 in 2020 would be derived from the mortality probability at age 65 in 2020, at age 66 in 2021, at age 67 in 2022, and so forth (G. L. Cairns 2013). Under this setting, the remaining expected years of an individual of a person at 1^{st} of January in the year t, assuming that the person was born on the 1^{st} of January of the year $t - x$, can be calculated by the *cohort life expectancy*:

$$e_{x,t}^{coh} = \frac{1}{2} + \sum_{k=0}^{\infty} \prod_{s=0}^{k} (1 - q_{x+s,t+s}) \tag{48}$$

The term $\frac{1}{2}$ is added based on the assumption that a person who dies within a given calendar year t has been alive for half of that year. "The probability that a person is alive at time $t + k$ is the product of survival probabilities $(1 - q_{x+s,t+s})$ for each year s between 0 and k, with the person not only ageing a year, but also moving to a new column in the mortality table" (AG 2020). Looking at Figure 38, which displays a matrix with forecasted mortality probabilities, the values of $q_{x,t}$ that would be inserted to derive the needed survival probabilities will move diagonally in the matrix.

This diagonal movement is not present in the calculation of the period life expectancy, and therefore the cohort effect is not incorporated. A period life table computes the lifespan of a population group using the mortality probabilities for a fixed time period. For example, the period life expectancy at age 65 in 2020 would use the mortality probabilities for 2020 for ages 65, 66, 67, and so forth.

$$e_{x,t}^{per} = \frac{1}{2} + \sum_{k=0}^{\infty} \prod_{s=0}^{k} (1 - q_{x+s,t}) \tag{49}$$

49, with the time indicator t remaining constant, suggests that the mortality probabilities do not evolve over the years. As a result, an incorrect estimation of life expectancy is created that can lead to miscalculations.

Period life expectancy would equal cohort life expectancy only in the highly improbable scenario that mortality rates by age remained constant over time. Period life expectancy assumes that the mortality rates from a single year (or a set of years) persist throughout the rest of a person's life (Ayuso, Bravo, and Holzmann 2021). This implies that any future changes to mortality rates would be ignored. Thus, period life expectancy is usually lower than cohort life expectancy because future enhancements in mortality rates are not accounted for (ONS 2023). This can be seen in Figure 14

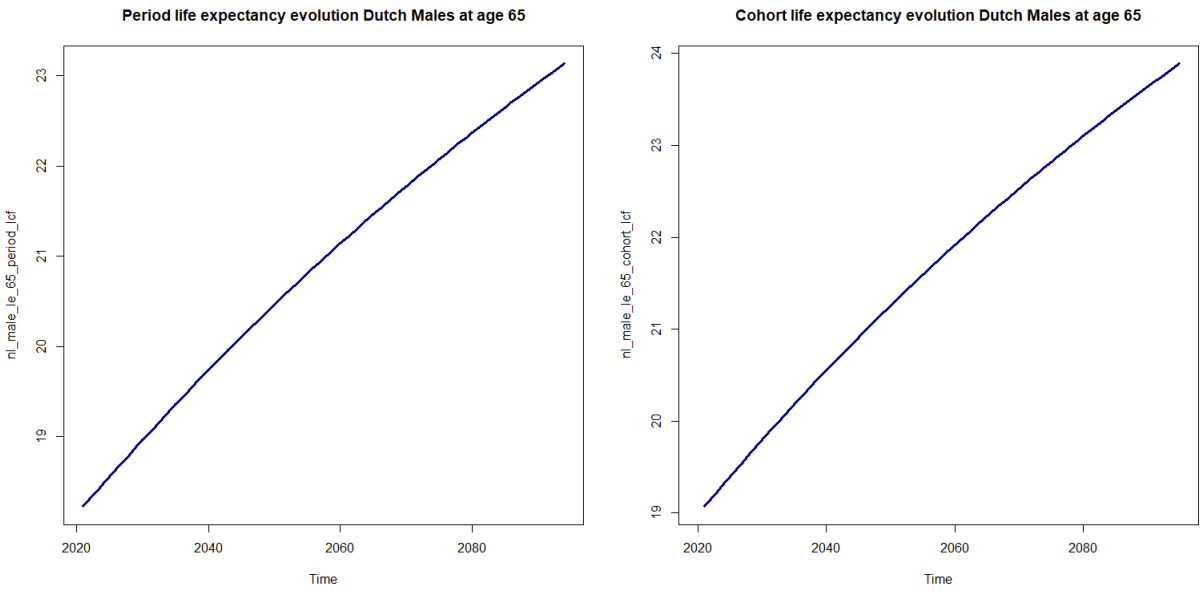

Figure 14: Forecasted evolution of period and cohort life expectancy in the LC model for Dutch males

7.3 Different Sampling periods

As can be read in AG 2022 annual Dutch and European mortality data from 1970 to 2019 are used to yield the Projections life table, which is why this period is mainly used throughout the thesis. The reason behind choosing this period is to create a large enough sample in order to produce more accurate results and simultaneously avoid periods from which mortality has deviated highly. The conclusion that can be deducted from Figure 15 is not surprising. The life expectancy at birth for the mortality data-set from 1980 to 2020 is shown higher than its counterparts which start from 1950, 1960 and 1970. This can be attributed to the fact that in the case of the 1980-2020 dataset the "worse" mortality rates observed in the former periods were ignored.

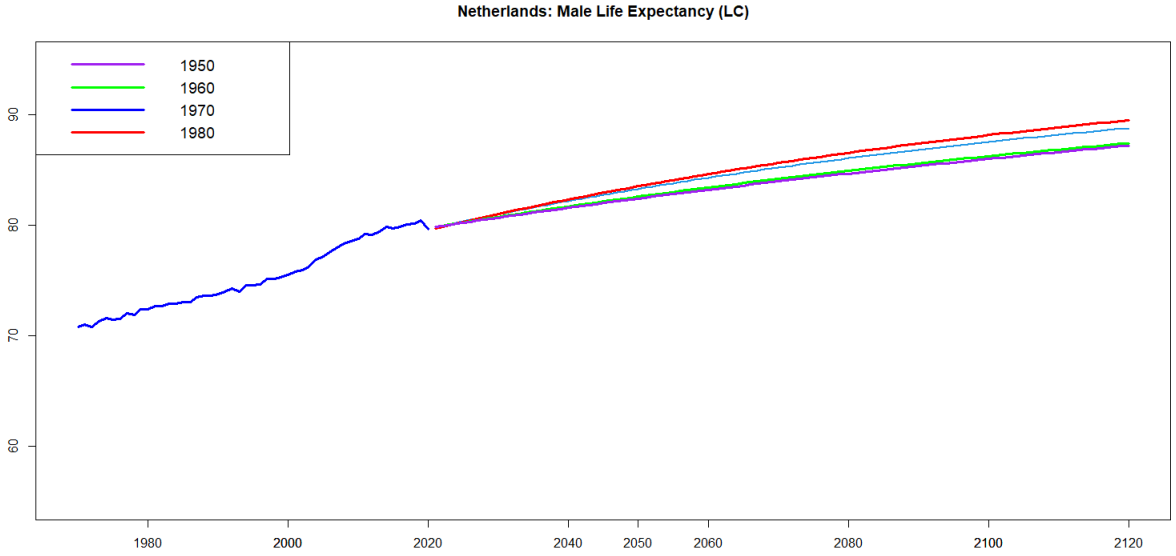

Figure 15: Historical and projected Dutch male life expectancy with 4 different starting fitting periods (Lee-Carter Model)

7.4 Life Expectancy single population models

First, κ_t is forecasted 100 years into the future for all models. As already mentioned in 7.1 the term $\boldsymbol{\iota_{t-x}}$ of the Renshaw-Haberman model is not extrapolated. After, combining the historical and projected performance of κ_t (see Figures 13,31,30), the mortality rates are produced in a similar manner. In Figures 32 and 33 (Appendix B), the expected improvement in the mortality rates for Dutch males at the age of 65 is depicted. In Figure 16 the mortality rates for the 1956 cohort in the Renshaw-Haberman model is shown, with the historical rates going up until 2021, where the cohort is aged 65 and future mortality rates are extrapolated, as the available data-set is dated up until 2021. The corresponding graphs for the remaining single population models are depicted in Figures 34 and 35.

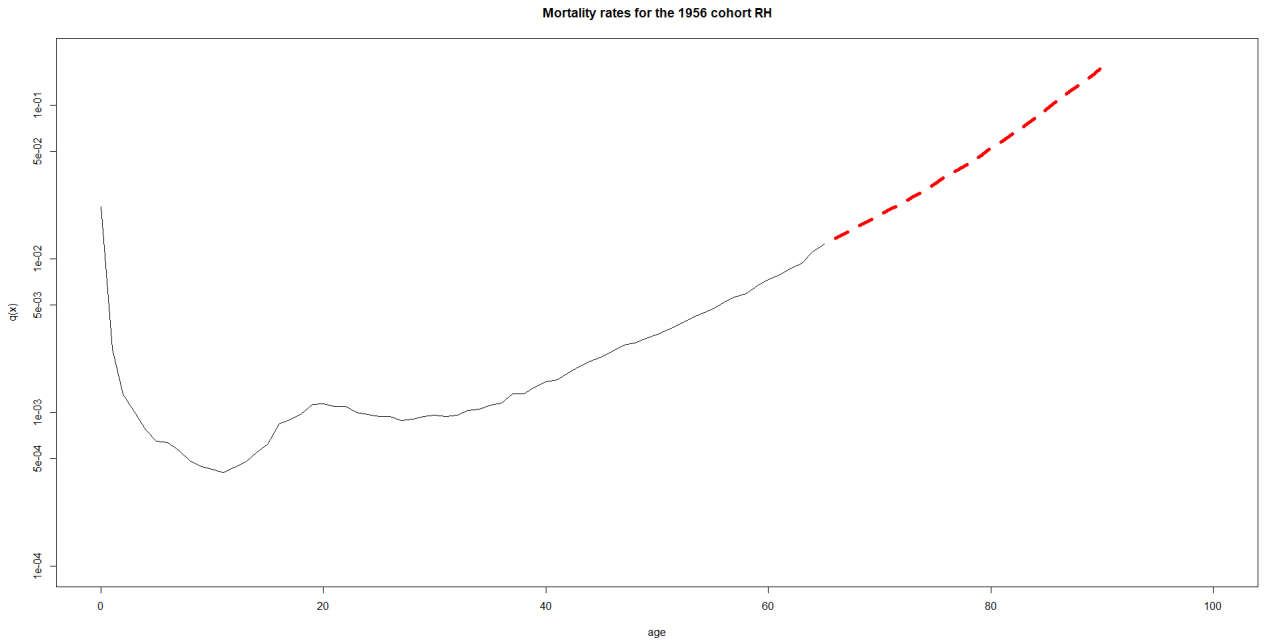

Figure 16: Historical and projected evolution of mortality rates in the Renshaw-Haberman model for Dutch males at the age of 65 (1956 cohort)

In order to yield the life expectancy in the different models, it is required to convert the mortality rates to mortality probabilities and produce the needed life-tables (G. A. Spedicato, Fcas, and Clemente 2021).

	Lee-Carter	Lee-Carter Poisson	Renshaw Haberman
Life Expectancy at 65	18.3	18.5	19.8

The table above presents the expected remaining years of Dutch males at age 65 for data from 1970 to 2020, with the Renshaw-Haberman model appearing more optimistic, as it indicates almost 2 additional remaining years of life expectancy.

A common assumption is that models with more parameters fit the data better. However, this could also be attributed to over-parametrization. To avoid this problem and compare different models, many researchers in the mortality field use information criteria. These criteria adjust the maximum likelihood criterion by adding a penalty for more parameters (A. M. Villegas, Kaishev, and Millossovich 2018). Two examples of these criteria are the Akaike Information Criteria (AIC) and Bayesian Information Criteria (BIC), which are defined as:

$$AIC = 2\nu - 2L \tag{50}$$

$$BIC = \nu \log K - 2L, \tag{51}$$

where lower values of AIC and BIC are preferred.

	Lee-Carter	Lee-Carter Poisson	Renshaw Haberman
Number of parameters	231	231	**460**
AIC	45062	44787	**39465**
BIC	46550	46275	**42429**

From the table above, we can conclude that the Renshaw-Haberman model scores the best in all criteria, which combined with the indicated prolonged life expectancy raise the question whether a cohort mortality model would be suitable for the Dutch society.

Table 17 depicts the evolution of cohort life expectancy for Dutch males aged 65 across the single population mortality models. In the Renshaw-Haberman model, cohort life expectancy experiences a significant "jump" in the period 2000 to 2020, which creates an important gap with the other two models. Also, it boasts the most optimistic number of expected remaining years, which amounts to around 26. On the other hand, Lee-Carter and Lee-Carter Poisson, with the latter accounting for higher values for the majority of the time period, experience a similar trend and eventually become almost identical.

Similar conclusions can be drawn by examining Figure 18 which shows the corresponding evolution of mortality rates. From 1970 to 2010 Renshaw-Haberman accounts for the lowest mortality rates. However, death rates experience an increase until 2040, from which point the mortality rates become significantly lower. It should be noted that Lee-Carter and Lee-Carter Poisson experience a smoother -almost identical- evolution across the years.

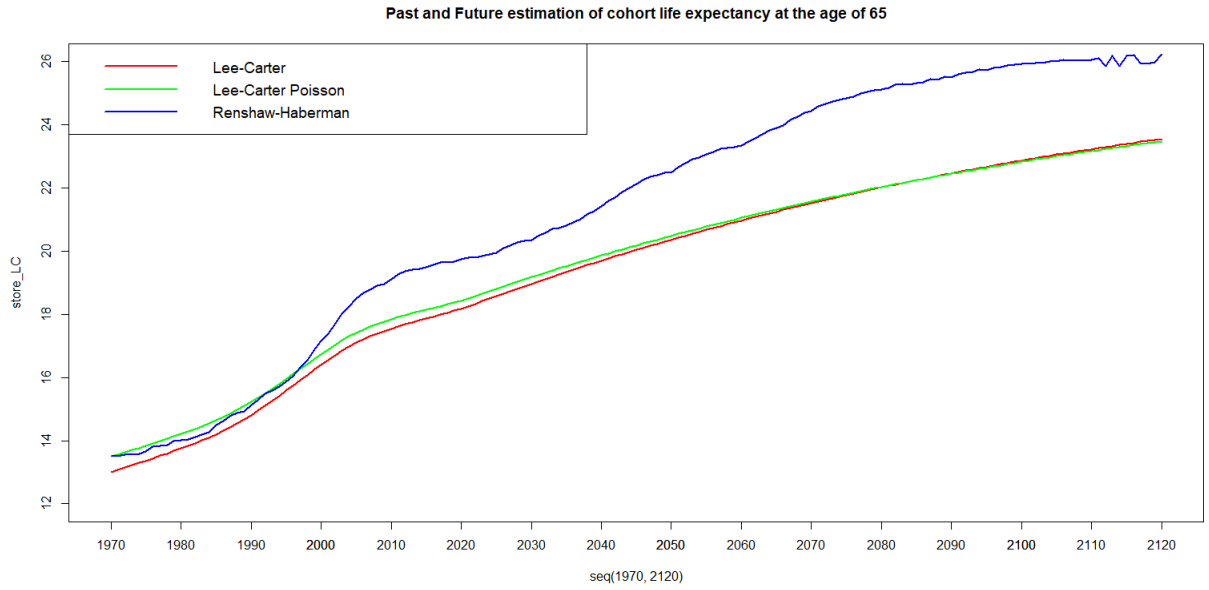

Figure 17: Evolution of past and projected estimation of cohort life expectancy for Dutch males aged 65 in the single population models

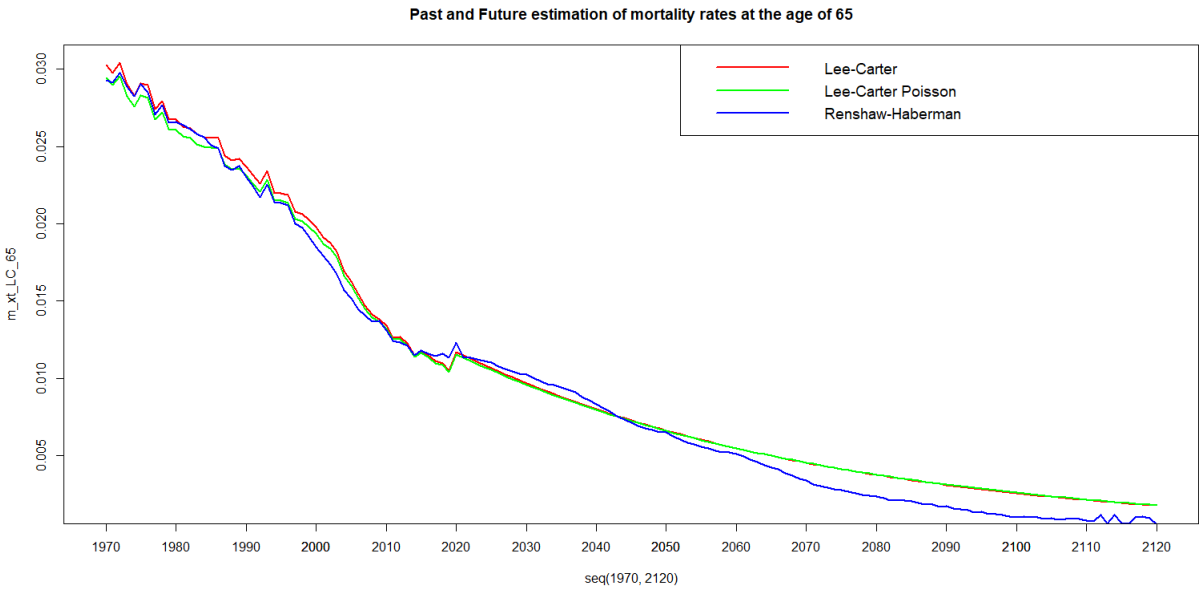

Figure 18: Evolution of past and projected estimation of mortality rates for Dutch males aged 65 in the single population models

7.5 Actuarial Present Value

It is important to examine how longevity risk affects pension payments by determining the actuarial present value (APV)[6] of a life annuity in the different models.

A life annuity involves a series of payments being made for as long as the insured individual remains alive. The comparison is conducted in terms of the APV, which is the expected value of the present value of a future payment stream contingent on the survival of the beneficiary. Essentially, it denotes the average monetary amount assured by the insurer to the policyholder. (G. Spedicato 2013).

$$\tilde{Z} = \begin{cases} \ddot{a}_{K+1} & \tilde{K_x} < n \\ \ddot{a}_n & \tilde{K_x} \geq n \end{cases}, \tag{52}$$

where $\tilde{K_x}$ represent the number of future years completed before mortality, while n accounts for the maximum years that the life annuity is active. In the examples shown below, the duration of the life annuity depends purely on the survival of the policy holder and does not expire. The assumption is that upon retirement, each beneficiary receives a single payment per year, subject to the condition of the policy holder being alive, with a constant risk-free interest rate of 2.55%.

Table 2 depicts how the annuity values for Dutch males and females aged 65 will change over four years in the future [7], using the Lee-Carter, Lee-Carter Poisson, and Renshaw-Haberman models. The increase in annuity values is related to the prediction of a more prolonged life expectancy in the future. This increase lies in the fact that with the decrease of mortality rates, there will be more annual payments to be made to the policy holders. Looking at Table 3, which shows the APVs for different ages in the year 2021, we can notice a decrease in the annuity values. This is due to the fact that annual payments are expected to take place for a smaller number of years as the age increases. In both tables, APVs for females account for higher values than their male counterparts, which is attributed to the higher life expectancy of the former. Last, in all situations, Renshaw-Haberman model produces the highest values of APVs, which can be attributed to the incorporation of the cohort term that accounts for increased estimated lifespan.

	Model	Male	Female
$\ddot{a}_{65}^{2021}$	LC	7.76	8.74
	LC Poisson	7.75	8.73
	RH	8.58	9.01
$\ddot{a}_{65}^{2026}$	LC	10.52	11.73
	LC Poisson	10.5	11.71
	RH	11.78	12.19
$\ddot{a}_{65}^{2031}$	LC	13.34	14.57
	LC Poisson	13.32	14.56
	RH	15	15.24
$\ddot{a}_{65}^{2036}$	LC	15.59	16.75
	LC Poisson	15.68	16.73
	RH	17.39	17.64

Table 2: APVs for both genders aged 65 across the years for the single population models.

[6]The calculation is conducted using the *lifecontingencies* R package.

[7]The fitting period for all models was 1970-2020, thus 2021 belongs to future time periods.

	Model	Male	Female
$\ddot{a}_{65}^{2021}$	LC	7.76	8.74
	LC Poisson	7.75	8.73
	RH	8.58	9.01
$\ddot{a}_{67}^{2021}$	LC	5.72	6.38
	LC Poisson	5.7	6.37
	RH	6.3	5.59
$\ddot{a}_{70}^{2021}$	LC	2.49	2.6
	LC Poisson	2.49	2.6
	RH	2.63	2.66

Table 3: APVs for both genders in the year 2021 for different ages for the single population models.

7.6 The Kannistö Method

Throughout the Thesis the data used by the models are obtained from the Human Mortality Database, as described in Section 6, for ages $X = \{0, 1, ..., 90\}$, which assumes 90 as the maximum attainable age by the individuals. The reason for choosing 90 as the upper bound in the age selection mainly lies on the fact that data beyond this point are either sparse or non-existent for some countries. In order to overcome this obstacle, the Kannistö is used to extrapolate mortality for the older ages. The same method has been employed by AG2014-2020 to determine mortality probabilities at high ages.

The set of ages used in estimation is $X^k = \{80, 81, ..., 90\}$ in order to extrapolate information for ages $\tilde{X} = \{91, 92, ..., 120\}$.

The mean of the ages on which the regression is based is:

$$\bar{y} = \frac{1}{n}\sum_{k=1}^{n} y_k = 85 \tag{53}$$

and the sum of differences:

$$\sum_{k=1}^{n}(y_k - \bar{y})^2 = 110 \tag{54}$$

The force of mortality for $\tilde{X}$ is calculated based on the following formula (AG 2014):

$$m_{x,t} = L(\sum_{k=1}^{n} w_{k,x} L^{-1}(m_{y_k,t})), \tag{55}$$

where :

$$\text{Ł}_x = \frac{1}{1 + e^{-x}} \tag{56}$$

$$\text{Ł}_x^{-1} = -\log(\frac{1}{x}) - 1 \tag{57}$$

$$w_{k,x} = \frac{1}{n} + \frac{(y_k - \bar{y})(x - \bar{y})}{\sum_{k=1}^{n}(y_k - \bar{y})^2} = \frac{1}{11} + \frac{(y_k - 85)(x - 85)}{110}, \tag{58}$$

where k refers to the ages from the estimation set and x to the high age that we want to obtain information for.

8 The cohort effect in the Dutch society: Double Renshaw-Haberman

The difference in the results between the models incorporating or not the cohort effect raises the question whether such a model should be employed for mortality projections in the Dutch society. In order to test this inquiry, similarly to the Lee-Carter setting, data will be drawn from an international setting to strengthen the forecasts. The new model that is going to be examined can be characterized as a double Renshaw-Haberman and its structure matches the dynamics of the AG model, which paves the way for constructive comparison.

8.1 Double Renshaw-Haberman : Model Description

Similarly to AG's setting, the force of mortality for the Netherlands is calculated as a sum of the European and Dutch forces of mortality by incorporating the cohort term. The double Renshaw-Haberman can be expressed as :

$$\log(m_{x,t}) = \log(m^{EU}_{x,t}) + \log(m^{NL}_{x,t}), \tag{59}$$

where:

$$\log(m^{EU}_{x,t}) = A_x + B^1_x K_t + B^0_x I_{t-x} \tag{60}$$

$$\log(m^{NL}_{x,t}) = \alpha_x + \beta^1_x \kappa_t + \beta^0_x \iota_{t-x} \tag{61}$$

The parameters in use have the same function as in the original Renshaw-Haberman described in 5.5, with the capital case parameters corresponding to the European super-poluation and the lowercase parameters pertaining to Dutch society. It is, also, worth noting that the data that are being inserted to the model have to be gender-specific.

For this setting data from the 14[8] are gathered from the period 1970 to 2018 and include ages 0 to 90.

8.2 Double Renshaw-Haberman : Estimating the parameters

The approach to fit the model follows a similar approach to the Li-Lee and can be described as a two-step Renshaw-Haberman model. First, the model is fit to the European data to obtain the super-population parameters. Subsequently, Δ is calculated as shown below:

$$\Delta = \log(m^{NL}_{x,t}) - \log(\hat{m}^{EU}_{x,t}) \tag{62}$$

$$\Delta = \log(\frac{D^{NL}_{x,t}}{E^{NL}_{x,t} \times \hat{m}^{EU}_{x,t}}), \tag{63}$$

where $D^{NL}_{x,t}$ and $E^{NL}_{x,t}$ refer to the raw data acquired from the Dutch data-set and $\hat{m}^{EU}_{x,t}$ accounts for the fitted values obtained from fitting the model to the European group. In (63) $E^{NL}_{x,t}$ is multiplied by $\hat{m}^{EU}_{x,t}$, which can be interpreted as an approximation of the expected deaths based on the super-population pattern. After obtaining the Dutch deviance, a final Renshaw-Haberman will be fit to Δ, where $D^{NL,\delta}_{x,t}$ is equal to the raw deaths from the mortality data-set and $E^{NL,\delta}_{x,t}$ is equal to the product of $E^{NL}_{x,t} * \hat{m}^{EU}_{x,t}$. A Poisson likelihood

[8]The same group as in the Li-Lee model

maximization approach is being utilized, while the same constraints as in 5.5.2 are employed (Hunt and A. Villegas 2015).

In Figure 19 the parameter evolution in the Double Renshaw-Haberman model is depicted. The interpretation of the plots requires attention, since the right side accounts for the parameter values obtained by fitting the model to Δ and this explains the unexpected look of the evolution. The most prominent feature of the parameter evolution for the Dutch deviance is the increasing trend of κ, which differs from the intuition that expects a downwards evolution. However, this does not pose a problem for the model, since the corresponding values of K_t^{EU} are significantly larger and experience an almost linear decreasing trend. B_x^1 experiences a steep decrease in the young ages and then smoothly approaches 0, whereas β_x^1 undergoes more variation, reaching even negative values, and plateaus after the age of 50, while the evolution of B_x^0 and β_x^0 is similar. I_{t-x} starts with its lowest values for the 1880 cohort and experiences a constant rising movement until approximately the 1950 cohort, from which point onwards undergoes a smooth decrease until the 2000 cohort, with its values being subjected to a small fluctuation without remarkable changes afterwards. Furthermore, the ι_{t-x} evolution for the Dutch deviance appears to be significantly stable in its values, which are concentrated close to 0 with the majority being negative. Last, A_x and α_x experience an increasing evolution. The former follows a smooth downwards trend until approximately the age of 15 and the undergoes a constant increasing trend, while experiencing the already observed jump in the age of 20. α_x starts with larger values than the European counterpart, experiences heavy fluctuations with a general decreasing trend until the age of 30 and then follows an increasing trend.

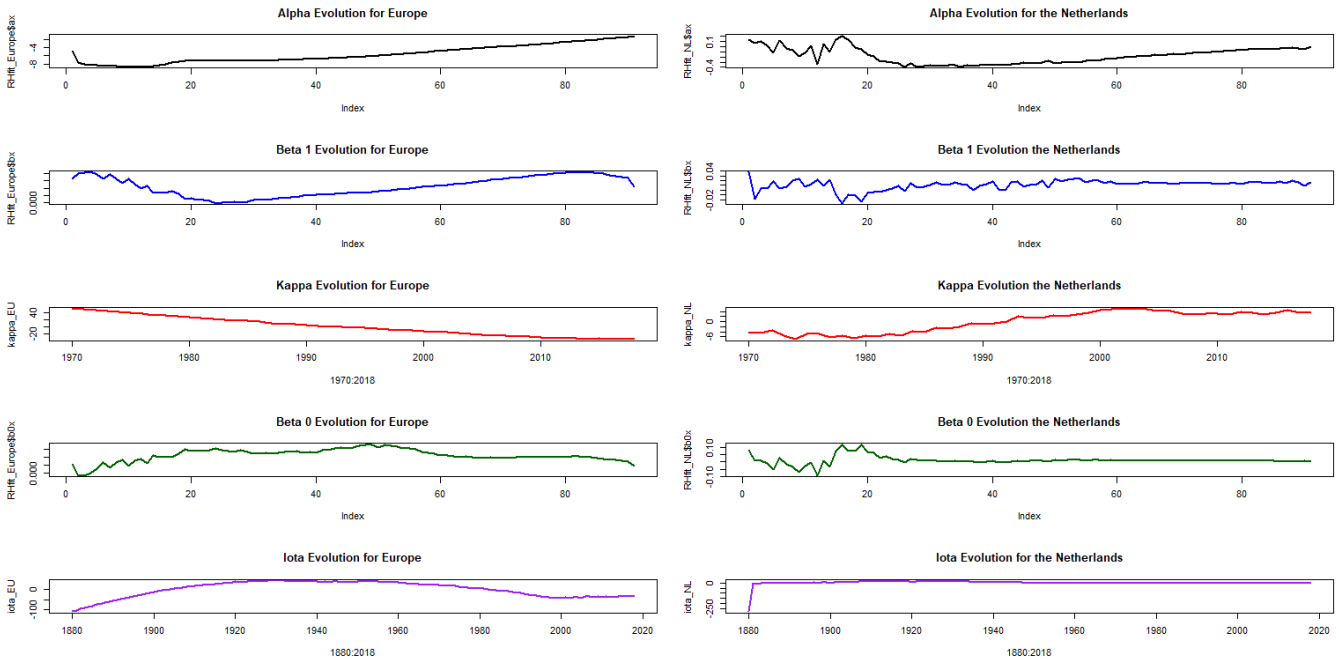

Figure 19: Parameter evolution for European and Dutch males in the double Renshaw-Haberman model

The abnormal, as opposed to the intuition facilitated, evolution of the parameters in the Dutch deviance should not be concerning. Figure 20 depicts the evolution of the sum of A_x and α_x that will be created, as can be seen in (59),(60),(61), and coincides with the expected evolution of the age-specific constant. Regarding the other terms, $\beta_x^{(1)}\kappa_t$ that refers to the Dutch population is the sum of $B_x^{(1)}K_t$ and $\beta_x^{(\delta,1)}\kappa_t^{\delta}$, with the same applying to $\beta_x^{(0)}\iota_{t-x}$. Therefore, the changes occur in terms of the resulting product and, thus, are not depicted, since the plots appear hectic and cannot be compared with the already observed figures.

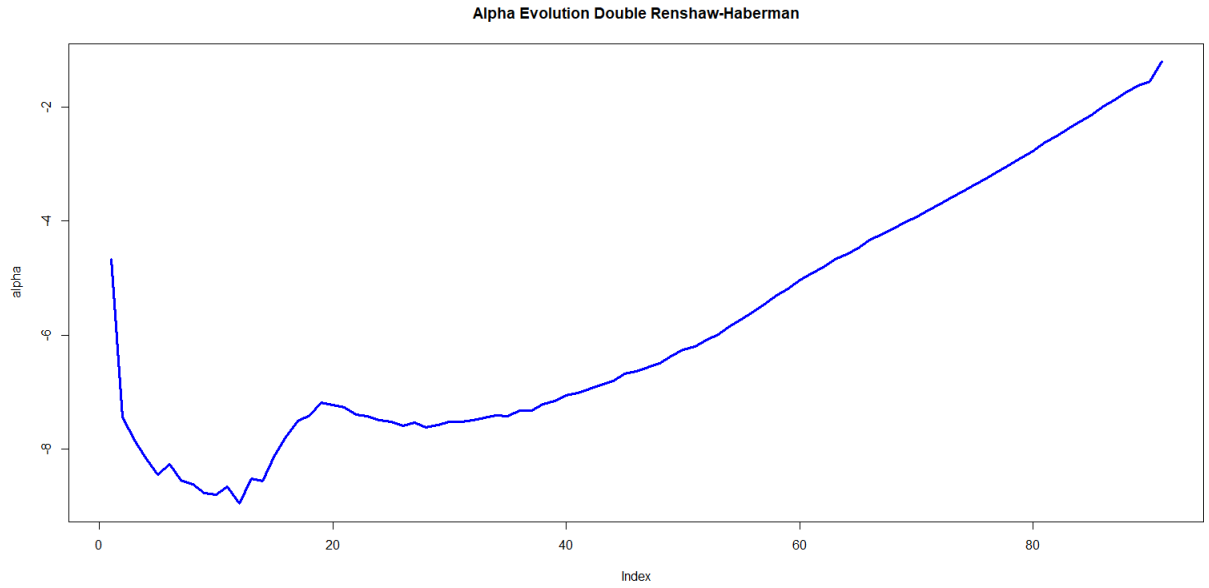

Figure 20: Evolution of A_x and α_x sum in the double Renshaw-Haberman model

8.3 Double Renshaw-Haberman : Forecasting

Having fit the model to the data, forecasting can be conducted. Following a similar approach as in the estimation process, K_t and κ_t are extrapolated into the future separately as ARIMA (0, 1, 0) (Random Walk with Drift). Only the time indices are forecasted in order to create a level playing field to compare the double Renshaw-Haberman with the corresponding AG model, which does not take into account the cohort term.

In Table 21 the evolution of the forecasted mean of the time indices, European and Dutch, is displayed. Their forecasted evolution follows a similar trend with evolution in the historical data.

For the purposes of forecasting, the force of mortality is estimated by inserting the parameters values of the fit data for $A_x, B_x^{(0)}, B_x^(1), I_{t-x}, \alpha_x, \beta_x^{(0)}, \beta_x^(1), \iota_{t-x}$, with the first four stemming from the European super-population and the latter from the Dutch specific group. Finally, in order to obtain the forecasted force of mortality separately the predicted values of K_t and κ_t are fit.

$$m_{x,t} = e^{A_x + B_x^1 K_t + B_x^0 I_{t-x}} \times e^{\alpha_x + \beta_x^1 \kappa_t + \beta_x^0 \iota_{t-x}} \tag{64}$$

After acquiring the force of mortality, the mortality probabilities can be calculated, as seen below (AG 2018). In the last step it is assumed that $m_{x+s,t+s} = m_{x,t} for\ 0 \leq s < 1$.

Figure 22 displays the forecasted cohort life expectancy of 65 year old Dutch males. The predicted period is 2019:2083, where 2083 is the last year that we have information regarding the cohort effect for that age. The expected remaining years experience an increasing trend, reaching approximately 25 additional years in 2083.

$$q_{x,t} = 1 - e^{-\int_0^1 m_{x+s,t+s}\, ds} = 1 - e^{-m_{x,t}} \tag{65}$$

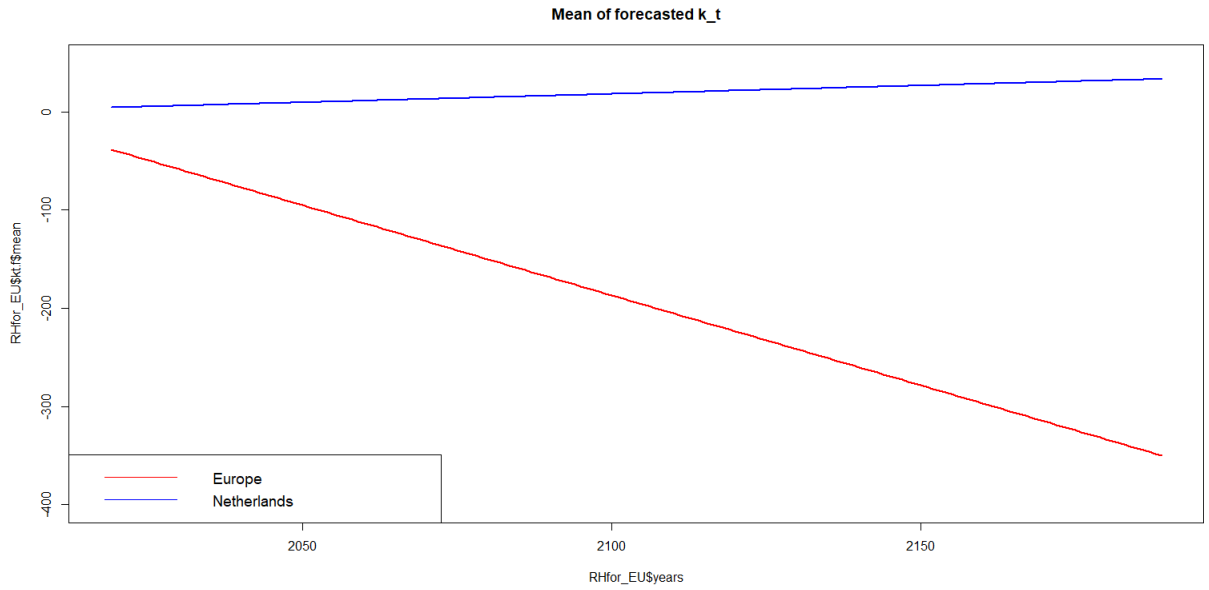

Figure 21: Evolution of the forecasted time index in the Double Renshaw-Haberman for Europe and Dutch males.

Figure 22: Cohort life expectancy for Dutch males aged 65 2019:2083 DRH 85% confidence interval

8.4 Actuarial Present Value

Following the same methodology as in the single population models, it is interesting to compare the newly introduced Double Renshaw-Haberman to its counterpart, the AG model, in terms of annuity values. Since the R libraries used before cannot be employed in this setting, the method of computing the market value of a life annuity described in (Hari et al. 2008) is implemented. It is assumed that the policyholder is guaranteed a nominal annual payment of 1, with the starting year being the year which the annuitant reaches the age of 65 and the last payment being made in the year the individual dies. As it can be deduced from the formulas below, the maximum age attainable by the policyholders is set to 120 and the force of mortality for the ages $\{91, 92, ..., 120\}$ has been extrapolated with the Kannistö method described in 7.6. Additionally, the interest rate is set at 2% and the APV is calculated with compound interest.

$$\ddot{a}_x = \sum_{\tau=\max[65-x,0]}^{120-x} \mathbb{E}[1_{(T_x \geq \tau]} P_0^{(\tau+1)} \tag{66}$$

$$\ddot{a}_x = \sum_{\tau=\max[65-x,0]}^{120-x} \mathbb{E}_t[{}_\tau p_{x,t}] \frac{1}{(1+r)^\tau} \tag{67}$$

$$\ddot{a}_x = \sum_{\tau=\max[65-x,0]}^{120-x} \exp(-\sum_{s=0}^{\tau-1} m_{x+s,t+s}) \frac{1}{(1+r)^\tau}, \tag{68}$$

where $P_0^{(\tau+1)}$ denotes the current market value of a zero-coupon bond with maturity date $\tau+1$, T_x accounts for the remaining lifetime of an annuitant aged x at the year of interest, ${}_\tau p_{x,t}$ is the probability that an x-year old will survive at least another τ years and $\mathbb{E}[1_{(T_x \geq \tau]}$ the expected value of one unit to be paid at time $\tau+1$ conditional on the survival of the annuitant.

Table 4 illustrates the anticipated changes in annuity values for Dutch individuals aged 65 in the forecasted year 2019 [9] in both the Double Renshaw-Haberman and AG models. The rise in annuity values corresponds to projections of extended life expectancy ahead. This upsurge is rooted in the expectation of declining mortality rates, resulting in more frequent annual payouts to policyholders. As anticipated with the general belief and the corresponding findings in 7.5, female annuities' values are higher than their male counterparts. For females, it is worth noting that for the years 2019 and 2024 AG produced higher annuity values before being surpassed by the corresponding DRH values. Additionally, the discrepancies for females range from 4% in 2019 to 6% in 2034. On the other hand, DRH produces the highest values in all years for males, with larger differences being recorded, ranging from 4% in 2019 to 15% in 2034, which is something to be taken into consideration for life insurers. Furthermore, Table 5 presents the Annuity Present Values (APVs) for various age groups in 2019, indicating a decline in annuity values. This decline stems from the anticipation of fewer years of annual payments as individuals age. Again, females exhibit higher APVs compared to males, reflecting their longer life expectancy. Similarly to Table 4 DRH boasts the larger APV values for males, whereas the AG accounts for the higher annuity values for the ages 65 and 75 in 2019.

[9] In this setting the fitting period was 1970-2018.

	Model	Male	Female
$\ddot{a}_{65}^{2019}$	DRH	8.35	9.25
	AG	7.97	9.65
$\ddot{a}_{65}^{2024}$	DRH	9.06	9.69
	AG	8.3	9.96
$\ddot{a}_{65}^{2029}$	DRH	9.88	10.33
	AG	8.64	10.28
$\ddot{a}_{65}^{2034}$	DRH	10.7	11.4
	AG	9	10.62

Table 4: APVs for both genders aged 65 across the years for the Double Renshaw-Haberman and AG

	Model	Male	Female
$\ddot{a}_{35}^{2019}$	DRH	5.28	5.52
	AG	3.83	4.55
$\ddot{a}_{45}^{2019}$	DRH	5.32	5.91
	AG	4.37	5.3
$\ddot{a}_{55}^{2019}$	DRH	6.15	6.79
	AG	5.41	6.75
$\ddot{a}_{65}^{2019}$	DRH	8.35	9.25
	AG	7.97	9.65
$\ddot{a}_{75}^{2019}$	DRH	5.13	5.98
	AG	4.88	6.11

Table 5: APVs for both genders in the year 2021 for different ages for the Double Renshaw-Haberman and AG.

8.5 Backtesting

In this section back-testing is employed in order to assess the newly introduced model's predictive ability.

First, the model is fitted on the 1970-2018 period. Figure 23 depicts the evolution of log mortality rates produced by the Double Renshaw-Haberman model (red) opposed to the realised rates (blue) for the forecasted years 2019, 2020, 2021. In every displayed period, log mortality rates in the DRH setting appear higher in the younger ages and they experience a softer drop as opposed to the realised rates. Beyond this point, they follow similar evolution with the line corresponding to DRH appearing lower. From the plots, it can be deducted that DRH produces a closer fit to the realised data in the year 2019. This could perhaps be due to the implications caused by Covid-19, which were not captured by the model.

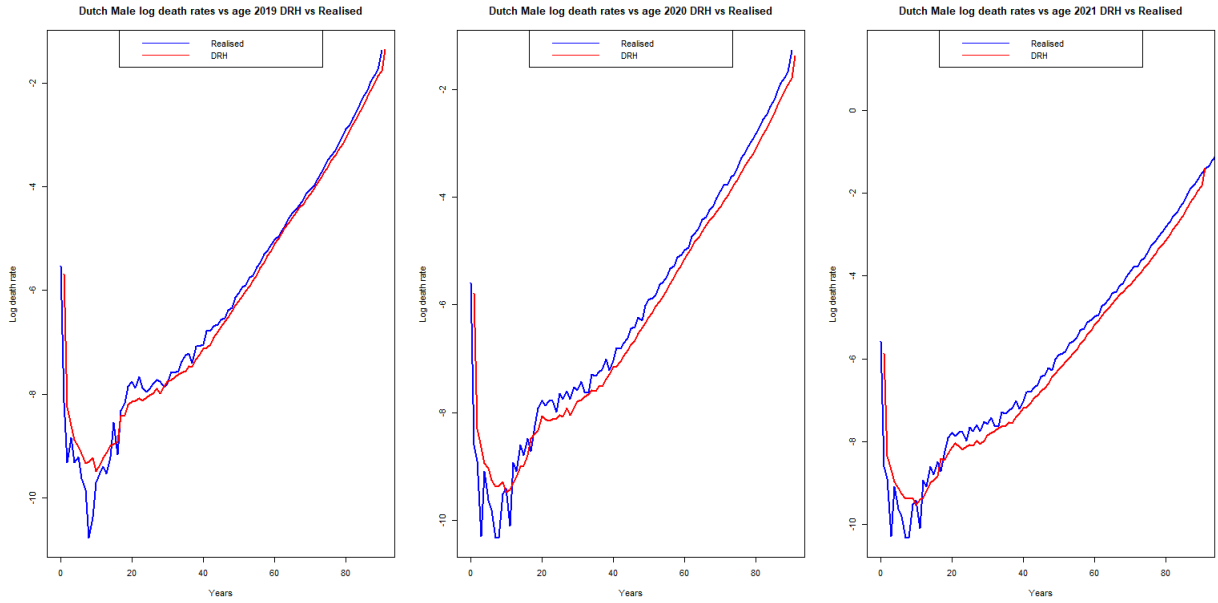

Figure 23: Log mortality rates in 2019-2021 Double Renshaw-Haberman and realised rates for Dutch males

Next, the testing period is extended to 10 years in order to facilitate an environment to compare the results produced by the DRH opposed the projections of the AG and LC models. In this setting the data used run from 1970 to 2008 and the testing interval runs from 2009 to 2018.

The forecasted deaths are computed as follows:

$$D_{x,t}^{model} = q_{x,t}^{model} \cdot E_{x,t} \tag{69}$$

Additionaly, the following metrics are employed in order to compare the models' ability to mimic the realised deaths as close as possible.

$$\frac{\sum_{t=2009}^{2018} \sum_{x=0}^{90} (D_{x,t}^{model} - D_{x,t}^{realised})}{\sum_{t=2009}^{2018} \sum_{x=0}^{90} D_{x,t}^{realised}} \tag{70}$$

$$\frac{\sum_{t=2009}^{2018}\sum_{x=0}^{90}|D_{x,t}^{model}-D_{x,t}^{realised}|}{\sum_{t=2009}^{2018}\sum_{x=0}^{90}D_{x,t}^{realised}} \tag{71}$$

Tables 6 and 7 display the performance of the three models Double Renshaw-Haberman, Lee-Carter and AG based on these metrics. In the relative difference setting (Eq. 70) LC accounts for the smallest difference (0.02) in males, since the values closer to 0 perform better, whereas DRH boasts the smallest for females (0.01). On the other hand, in the absolute difference setting (Eq. 71) DRH performs best for both sexes. It can be concluded that in this back-testing period of 10 years, DRH out-performed the other two models in the concept of predicting mortality.

Figure 24 displays the forecasted mortality by the three models and the realised deaths for Dutch males. Although, DRH out-performed its competitors, it did not achieve the best results in a year, with the first place belonging to AG. On the other hand, in Figure 45 (see Appendix B) DRH performs best in 6 of the 10 years.

Figure 25 displays the performance of the models on the predicting period life expectancy for 65 year old Dutch males. In this setting, the "realised" period life expectancy is found by calculating the force of mortality by $m_{x,t} = \frac{D_{x,t}^{real}}{E_{x,t}^{real}}$ and then obtaining the mortality probabilities, as seen in 65. It can be deduced from the plot that DRH performs best in the period 2009-2014, giving its place to AG for the remaining years. An opposite evolution can be noted for females in Figure 45, where DRH performs best in the period 2015-2018.

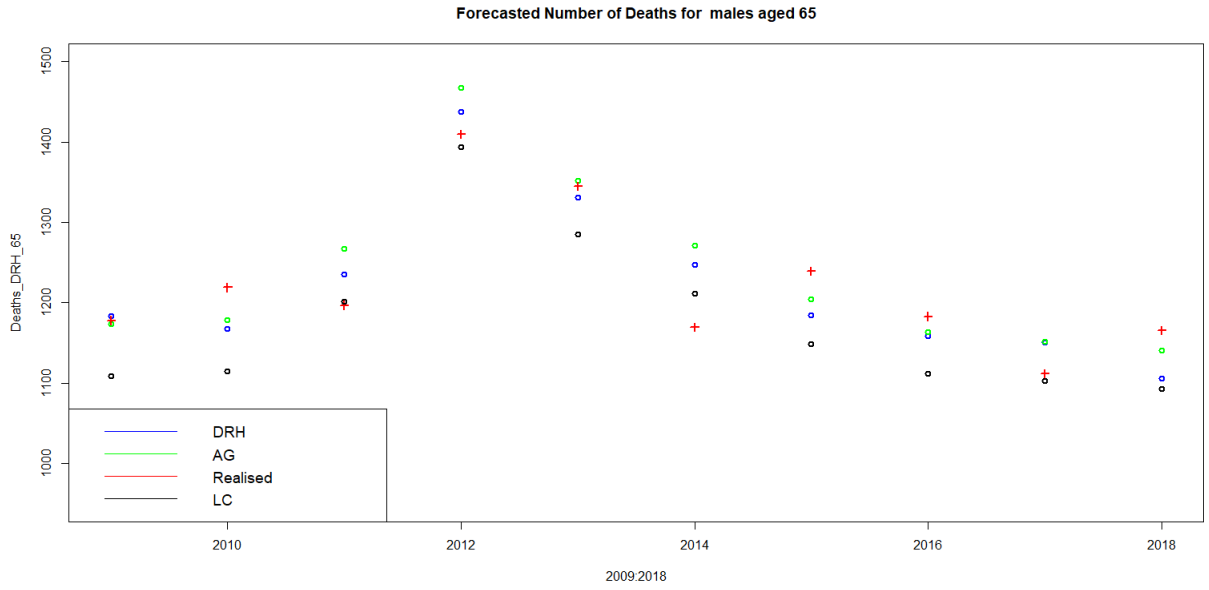

Figure 24: Forecasted number of deaths for LC, AG, DRH models and the realised deaths in the period 2009-2018 for 65 year old Dutch males

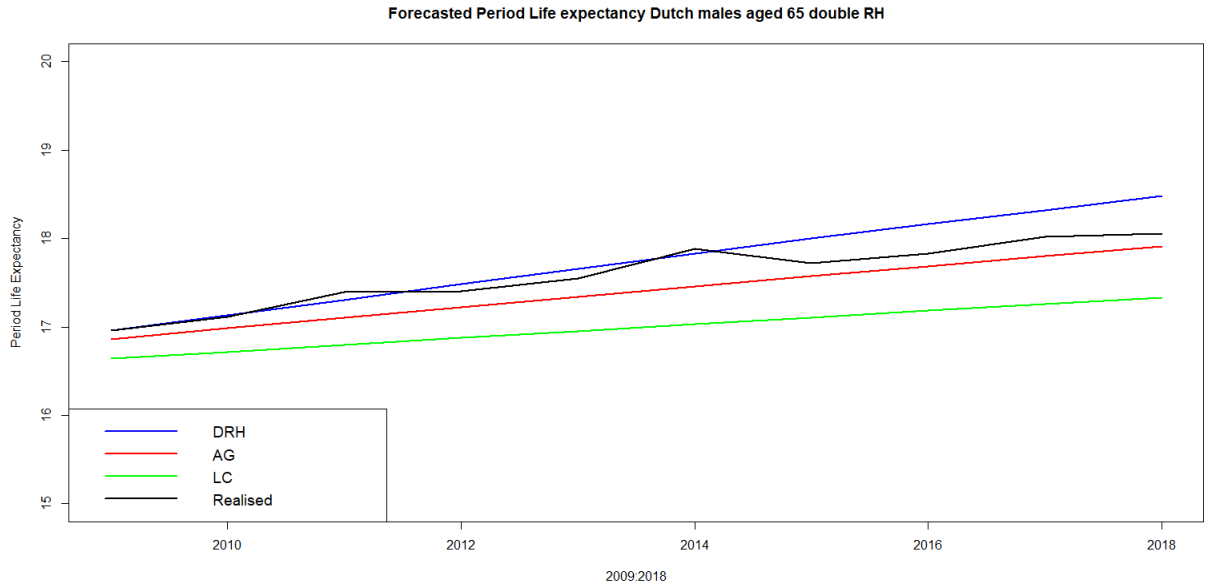

Figure 25: Forecasted period life expectancy LC, AG, DRH models and the realised period life expectancy in the period 2009-2018

Model	Male	Female
DRH	-0.06	**0.01**
LC	**0.02**	-0.14
AG	-0.03	0.15

Table 6: Relative difference for all deaths in the period 2009-2018 for DRH, AG and LC for ages 0-90, as shown in Equation 70

Model	Male	Female
DRH	**0.07**	**0.04**
LC	0.1	0.12
AG	0.08	0.15

Table 7: Absolute difference for all deaths in the period 2009-2018 for DRH, AG and LC for ages 0-90, as shown in Equation 71

To further test the performance of the newly introduced Double Renshaw-Haberman, the out of sample accuracy is going to be evaluated by Mean Squared Error (MSE) 72 independently for each gender (Scognamiglio and Marino 2023).

$$MSE_i = \frac{1}{|T||X|} \sum_{t \in T} \sum_{x \in X} (q_{x,t,i} - \hat{q}_{x,t,i})^2 \tag{72}$$

The MSE distribution over age is calculated as:

$$MSE_{x,i} = \frac{1}{|T|} \sum_{t \in T} (q_{x,t,i} - \hat{q}_{x,t,i})^2 \tag{73}$$

The set T refers to the backtesting period used for comparison, $T = \{2009, ..., 2018\}$ and $|T|$ represents the total number of years used, thus $|T| = 10$. Similarly, X represents the set of ages used in testing, $X = \{0, 1, ..., 90\}$ and therefore $|X| = 91$.

As can be seen in Table 8, DRH outperforms the LC and AG model in both sexes by achieving the lowest MSE, which further highlights DRH's out-of-sample performance.

The MSE distribution over age of the models is presented in Figures 26 and 27 is presented in order to investigate further the backtesting performance of the models. For display purposes MSE is depicted in log scale. All models experience similar trends in both genders. First, MSE undergoes a steep decrease for the young ages, while starting higher at age 0. Beyond this point, the evolution is constantly increasing while undergoing fluctuations. As the individuals become older, MSE approaches more closely to 0.

Model	Male	Female
DRH	**0.5503**	**1.4831**
LC	2.7720	3.3236
AG	3.5451	4.1451

Table 8: Gender-specific MSE for each model, as shown in Equation 72. Values are being displayed in 10^{-5}

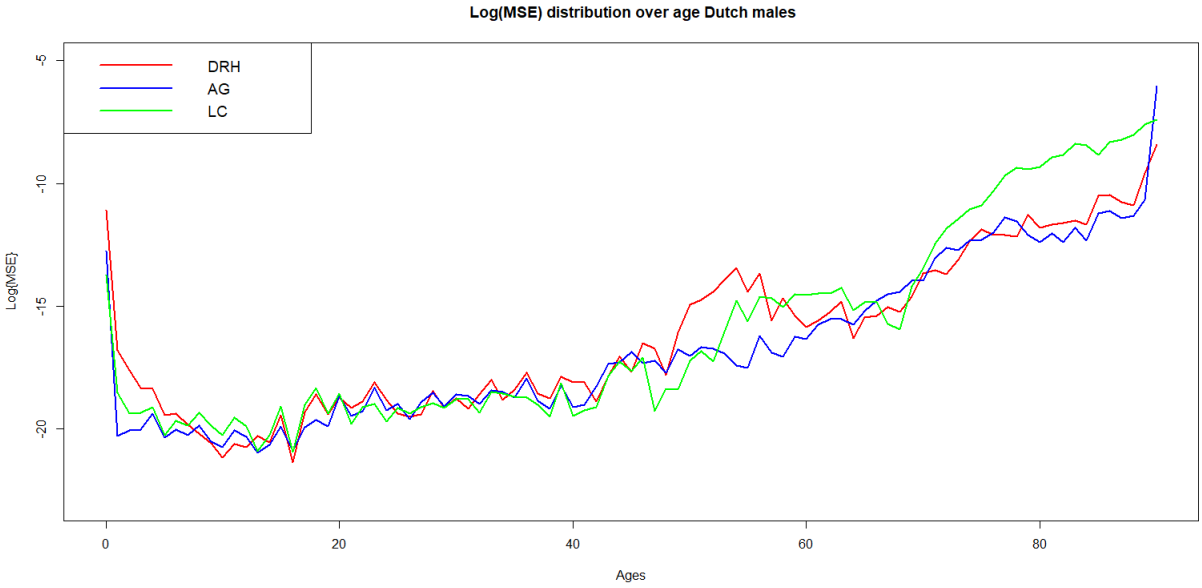

Figure 26: Log(MSE) distribution over age for Dutch males for the three models

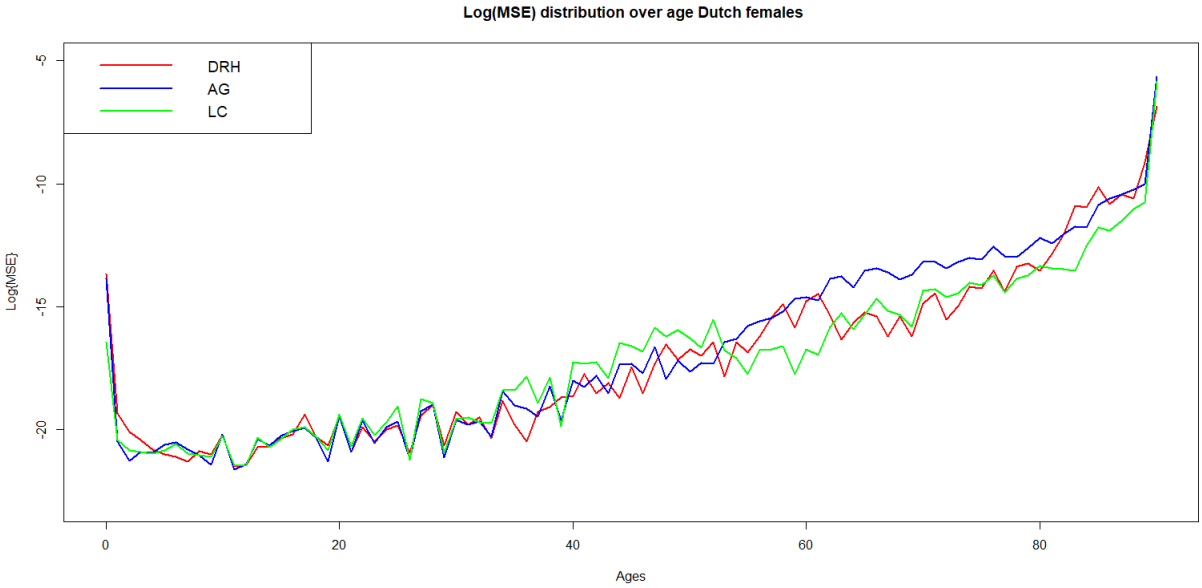

Figure 27: Log(MSE) distribution over age for Dutch females for the three models

9 Conclusion

This thesis embarked on a comprehensive examination of mortality projection models within the context of the Dutch society, culminating in the introduction of the Double Renshaw-Haberman model. By systematically reviewing, comparing, and implementing a variety of mortality models, including the Lee-Carter model and its extensions, this study has illuminated the complexities inherent in predicting mortality rates but has also underscored the critical importance of innovation and adaptation in mortality modeling methodologies. Section 5 sets the stage for technical and qualitative comparison of the models. The examination starting from the benchmark Lee-Carter and continuing with its extensions allows the reader to comprehend why certain modifications were introduced and what is their purpose on projecting mortality.

The core of this investigation underscored the paramount importance of accurately forecasting mortality rates. The Lee-Carter model and its subsequent adaptations have served as foundational elements in this pursuit. However, the introduction and application of the Double Renshaw-Haberman model can mark a pivotal starting point for future research regarding the implementation of the cohort effect into mortality modelling.

In Section 7, while comparing single population models, the results indicated that Renshaw-Haberman provided a better fitting to the data. This led to the question whether such a model could be implemented to modern practices. Following the steps of Li-Lee and AG, where a type of double Lee-Carter is applied, Double Renshaw-Haberman with the same European super-population was introduced in Section 8. The model outperformed the Lee-Carter and AG models in the back-testing period of 2009-2018 in forecasting the number of deaths and achieved the lowest MSE in both genders. The newly introduced model notes the necessity of incorporating cohort effects into mortality forecasts to better mirror real-world demographic shifts and trends. It suggests a paradigm shift towards more dynamic and nuanced modeling techniques that can adapt to and reflect complex societal changes. Modifications that are country-specific can not only enhance the precision of mortality forecasts but will, also, align with observed demographic trends and shifts within the mortality data.

More accurate mortality forecasting has a direct impact on pricing strategies, risk assessment, and long-term financial stability for insurance firms, especially life insurers and annuity providers. Accurate mortality estimates enable insurers to enhance their competitive advantage and meet their policyholder obligations by facilitating more efficient premium structuring, prudent reserve allocation, and investment strategy optimization.

Furthermore, the societal implications of improved mortality projections cannot be overstated. Policymakers may better anticipate demographic changes by using more accurate models, which will help them make decisions on social security, healthcare, and retirement planning. This highlights the advantages of sophisticated mortality modeling for both people and society as a whole. For individuals, this translates into more dependable life insurance products and maybe more advantageous premium costs.

In conclusion, this thesis extends beyond academic theory in mortality projections, offering practical insights and methods useful in actuarial science, insurance, and public policy. It introduces the Double Renshaw-Haberman model, which effectively incorporates cohort effects, significantly improving our ability to predict demographic changes. This research not only provides valuable information for practitioners but also lays the groundwork for further studies in mortality projections. It highlights the importance of continuous exploration of mortality within the context of global demographic shifts, technological progress, and changing societal norms.

10 Recommendations

The introduction and analysis of the Double Renshaw-Haberman model in the context of Dutch mortality data have highlighted its potential benefits, particularly in capturing cohort effects and improving the accuracy of mortality forecasts. However, like all models, it presents opportunities for refinement and areas that warrant further investigation. The following recommendations aim to guide future research and practical applications of this model:

1. Mortality Smoothing

Incorporating smoothing techniques, as detailed in (Currie, Durbán, and Eilers 2004a), into the Double Renshaw-Haberman model can address some of its inherent limitations by refining its predictive capabilities. Specifically, the application of P-splines (Currie, Durbán, and Eilers 2004b) allows for a more nuanced handling of mortality data, enabling the model to adapt more fluidly to underlying demographic trends and irregularities in the data. This flexibility is crucial for capturing the cohort effects with greater accuracy and mitigating the impact of overdispersion, a common challenge in mortality data analysis.

The smoothing process, as a natural extension of the modeling framework, facilitates a more robust forecasting mechanism. By treating future values as missing data within the smoothing framework, the model can extend its predictive horizon with a foundation that is both statistically sound and practically informative. This approach also allows for the model to incorporate and forecast based on both one-dimensional and two-dimensional data, enhancing its applicability across different demographic studies.

For future research directions, it's recommended to explore the integration of P-splines in the Double Renshaw-Haberman model further. This exploration could involve comparing the effectiveness of different orders of penalties within the P-spline framework to ascertain the most suitable for mortality forecasting. Additionally, investigating the model's adaptability to incorporate real-time data sources and emerging trends could provide valuable insights for more dynamic and responsive mortality forecasts. Such advancements would not only augment the model's predictive accuracy but also enhance its utility for insurance companies, policymakers, and demographic researchers aiming to devise strategies and policies informed by nuanced mortality projections.

2. Model Customization and Exploring Extensions

Given the variance in mortality trends and the influence of regional health policies, lifestyle factors, and socioeconomic conditions, it's essential to consider these elements in the model's application. Future studies should explore the customization of the Double Renshaw-Haberman model to reflect these variables more accurately. Incorporating country-specific health indicators and socioeconomic data could refine the model's forecasts, making them more relevant for local insurance markets and policy planning.

Current models, including the Double Renshaw-Haberman, primarily focus on age as the central variable in mortality projections. However, other indicators, such as health status, lifestyle factors, and environmental conditions, could provide valuable insights into mortality trends. Future research should consider these alternative indicators, possibly integrating them into the existing model framework to offer a more nuanced understanding of mortality dynamics, thus introducing valuable extensions to the Double Renshaw-Haberman model.

3. Integration of Big Data and Machine Learning as a tool in extending DRH

The evolution of big data and machine learning presents a significant opportunity to enhance the functionality and predictive accuracy of the Double Renshaw-Haberman model. As the healthcare industry becomes increasingly awash with vast amounts of data from diverse sources such as electronic health records, genetic testing, and wearable technology, the potential to refine mortality projections through advanced analytics

grows exponentially (Beam and Kohane 2018). Machine learning algorithms, particularly those high on the machine learning spectrum like deep learning models, are designed to process and learn from this data directly, identifying intricate patterns and correlations that may elude traditional statistical methods. By leveraging these capabilities, the Double Renshaw-Haberman model could be adapted to automatically adjust its parameters based on new, multidimensional data inputs, enhancing its precision and adaptability in forecasting mortality rates.

The integration of machine learning into the Double Renshaw-Haberman model appears as the natural next step to the traditional statistical approaches. In the modern data-rich environment, the ongoing evolution of such techniques can serve as a valuable tool in successfully capturing alternative indicators and providing the model with data of such newly introduced variables.

4. Alternative fitting of the cohort term.

In this application, the cohort effect ι_{t-x} is being fitted and simulated using ARIMA (1,0,0). Different approaches on the estimation of the cohort term can bring more accuracy to the results, as has already be seen with the time index κ_t.

11 References

References

AG, Prognosetafel (2014). "Koninklijk Actuarieel Instituut". In.

— (2018). "Koninklijk Actuarieel Instituut". In.

— (2020). "Koninklijk Actuarieel Instituut". In.

— (2022). "Koninklijk Actuarieel Instituut". In.

Antonio, Katrien et al. (Dec. 2017). "Producing the Dutch and Belgian mortality projections: A stochastic multi-population standard". English. In: *European actuarial journal* 7.2, pp. 297–336. ISSN: 2190-9733. DOI: 10.1007/s13385-017-0159-x.

Ayuso, Mercedes, Jorge M. Bravo, and Robert Holzmann (2021). "Getting life expectancy estimates right for pension policy: period versus cohort approach". In: *Journal of Pension Economics and Finance* 20.2, pp. 212–231. DOI: 10.1017/S1474747220000050.

Beam, Andrew L. and Isaac S. Kohane (Apr. 2018). "Big Data and Machine Learning in Health Care". In: *JAMA* 319.13, pp. 1317–1318. ISSN: 0098-7484. DOI: 10.1001/jama.2017.18391. eprint: https://jamanetwork.com/journals/jama/articlepdf/2675024/jama_beam_2018_vp_170174.pdf. URL: https://doi.org/10.1001/jama.2017.18391.

Bergeron-Boucher, Marie-Pier and Søren Kjærgaard (2022). "Mortality forecasting at age 65 and above: an age-specific evaluation of the Lee-Carter model". In: *Scandinavian Actuarial Journal* 2022.1, pp. 64–79. DOI: 10.1080/03461238.2021.1928542. eprint: https://doi.org/10.1080/03461238.2021.1928542. URL: https://doi.org/10.1080/03461238.2021.1928542.

Brouhns, Natacha, Michel Denuit, and Jeroen K. Vermunt (2002). "A Poisson log-bilinear regression approach to the construction of projected lifetables". In: *Insurance: Mathematics and Economics* 31.3, pp. 373–393. ISSN: 0167-6687. DOI: https://doi.org/10.1016/S0167-6687(02)00185-3. URL: https://www.sciencedirect.com/science/article/pii/S0167668702001853.

Cairns, Andrew et al. (Mar. 2007a). "A Quantitative Comparison of Stochastic Mortality Models Using Data From England Wales and the United States". In: *North American Actuarial Journal* 13. DOI: 10.2139/ssrn.1340389.

— (Mar. 2007b). "A Quantitative Comparison of Stochastic Mortality Models Using Data From England Wales and the United States". In: *North American Actuarial Journal* 13. DOI: 10.2139/ssrn.1340389.

Cairns, George Lindsay (2013). "A Bayesian approach to modelling mortality, with applications to insurance". In: *PhD thesis, University of Glasgow*.

Chiang, Chin Long and World Health Organization (1979). "Life table and mortality analysis / Chin Long Chiang". In: jpn published by: Tokyo : Institute of Actuaries of Japan.

Currie, Iain, María Durbán, and Paul Eilers (Dec. 2004a). "Smoothing and Forecasting Mortality Rates". In: *Statistical Modelling* 4. DOI: 10.1191/1471082X04st080oa.

— (Dec. 2004b). "Smoothing and Forecasting Mortality Rates". In: *Statistical Modelling* 4. DOI: 10.1191/1471082X04st080oa.

Edwards, Matthew (2020). "What is the difference between longevity and mortality?" In: URL: https://www.actuaries.org.uk/news-and-insights/news/what-difference-between-longevity-and-mortality#:~:text=If%20mortality%20increases%2C%20they%20pay%20out%20more%20than,discussed%20above%20end%20up%20being%20greater%20than%20assumed..

Hari, N. et al. (2008). "Longevity risk in portfolios of pension annuities". English. In: *Insurance Mathematics Economics* 42.2, pp. 505–519. ISSN: 0167-6687.

Hatzopoulos, P. and S. Haberman (Sept. 2015). "Modeling trends in cohort survival probabilities". In: *Insurance: Mathematics and Economics* 64. © 2015, Elsevier. Licensed under the Creative Commons Attribution-NonCommercial-NoDerivatives 4.0 International http://creativecommons.org/licenses/by-nc-nd/4.0/, pp. 162–179. ISSN: 0167-6687. DOI: 10.1016/j.insmatheco.2015.05.009. URL: https://openaccess.city.ac.uk/id/eprint/12162/.

Hobcraft, John, Jane Menken, and Samuel Preston (Feb. 1982). "Age, Period, and Cohort Effects in Demography: A Review". In: *Population index* 48, pp. 4–43. DOI: 10.2307/2736356.

Human (Mortality Database). In: *Max Planck Institute for Demographic Research, University of California, Berkeley, and French Institute for Demographic Studies,27/12/2023*. URL: www.mortality.org.

Hunt, Andrew and Andrés Villegas (May 2015). "Robustness and convergence in the Lee-Carter model with cohort effects". In: *Insurance: Mathematics and Economics* 64. DOI: 10.1016/j.insmatheco.2015.05.004.

Institute and Faculty of Actuaries (2007). "CMI: Stochastic projection methodologies: Lee-Carter model features, example results and implications". In: *CMI Working Paper 25*. URL: %7Bhttp://www.actuaries.org.uk/research-and-resources/pages/cmi-working-paper-25%7D.

Lee, Ronald (Jan. 2000). "The Lee-Carter Method for Forecasting Mortality, with Various Extensions and Applications". In: *North American Actuarial Journal* 4. DOI: 10.1080/10920277.2000.10595882.

Lee, Ronald and Lawrence R. Carter (1992). "Modeling and forecasting U. S. mortality". In: *Journal of the American Statistical Association* 87, pp. 659–671. URL: https://api.semanticscholar.org/CorpusID:29804325.

Levendis, John (Jan. 2018). *Time Series Econometrics: Learning Through Replication*. ISBN: 978-3-319-98281-6. DOI: 10.1007/978-3-319-98282-3.

Li, Huijing, Rui Zhou, and Min Ji (2023). "Nonlinear Modeling of Mortality Data and Its Implications for Longevity Bond Pricing". In: *Risks* 11.12. ISSN: 2227-9091. DOI: 10.3390/risks11120207. URL: https://www.mdpi.com/2227-9091/11/12/207.

Li, Nan and Ronald Lee (Sept. 2005a). "Coherent Mortality Forecasts for a Group of Population: An Extension of the Lee–Carter Method". In: *Demography* 42, pp. 575–94. DOI: 10.1353/dem.2005.0021.

— (2005b). "Coherent Mortality Forecasts for a Group of Populations: An Extension of the Lee-Carter Method". In: *Demography* 42.3, pp. 575–594. ISSN: 00703370, 15337790. URL: http://www.jstor.org/stable/4147363 (visited on 10/03/2023).

ONS, Office for National Statistics (2023). "Period and Cohort Life expectancy explained". In: *ONS website*.

Pitacco, E. et al. (2009). "Modelling Longevity Dynamics for Pensions and Annuity Business". In: URL: https://api.semanticscholar.org/CorpusID:150532568.

Renshaw, A.E. and S. Haberman (June 2006). "A Cohort-Based Extension to the Lee-Carter Model for Mortality Reduction Factors". In: *Insurance: Mathematics and Economics* 38, pp. 556–570. DOI: 10.1016/j.insmatheco.2005.12.001.

Scognamiglio, Salvatore and Mario Marino (Aug. 2023). "Backtesting stochastic mortality models by prediction interval-based metrics". In: *Quality & Quantity: International Journal of Methodology* 57.4, pp. 3825–3847. DOI: 10.1007/s11135-022-01537-. URL: https://ideas.repec.org/a/spr/qualqt/v57y2023i4d10.1007_s11135-022-01537-z.html.

Spedicato, Giorgio (Nov. 2013). "The lifecontingencies Package: Performing Financial and Actuarial Mathematics Calculations in R". In: *Journal of statistical software* 55. DOI: 10.18637/jss.v055.i10.

Spedicato, Giorgio Alfredo, Fsa Cspa C.Stat Fcas, and Ph.D Gian Paolo Clemente (2021). "Mortality projection using lifecontingencies , demography and StMoMo packages". In: URL: https://api.semanticscholar.org/CorpusID:245019182.

Stevens, R.S.P., A.M.B. De Waegenaere, and B. Melenberg (2011). "Longevity Risk and Natural Hedge Potential in Portfolios Of Life Insurance Products: The Effect of Investment Risk". English. In: CentER Discussion Paper 2011-036.

Villegas, Andrés M., Vladimir K. Kaishev, and Pietro Millossovich (2018). "StMoMo: An R Package for Stochastic Mortality Modeling". In: *Journal of Statistical Software* 84.3, pp. 1–38. DOI: 10.18637/jss.v084.i03. URL: https://www.jstatsoft.org/index.php/jss/article/view/v084i03.

Villegas Ramirez, Andres (2015). "Mortality: modelling, socio-economic differences and basis risk". In: Chapter 2 previously published as: Villegas, A. M., Haberman, S. (2014) On the modelling and forecasting of socio-economic mortality differentials: an application to deprivation and mortality in England. North American Actuarial Journal 18 (1), 168-193. doi:10.1080/10920277.2013.866034. Chapter 6 previously published as: Hunt, A., Villegas, A.M., 2015. Robustness and convergence in the Lee-Carter model with cohort effects. Insurance: Mathematics and Economics 64 186-202 doi:10.1016/j.insmatheco.2015.05.004. URL: https://openaccess.city.ac.uk/id/eprint/13574/.

Wikipedia contributors (2022). *Fan chart (time series)*. [Online; accessed 24-January-2024]. URL: https://en.wikipedia.org/wiki/Fan_chart_(time_series).

Willets, R. C. (2004). "The Cohort Effect: Insights and Explanations". In: *British Actuarial Journal* 10.4, pp. 833–877. DOI: 10.1017/S1357321700002762.

A Definitions/Derivations

Central Death rate and force of mortality

The central death rate m_x represents the average number of deaths per person aged x and is calculated by :

$$m_x = \frac{\text{number of deaths}}{\text{time spent alive at risk}},$$

whereas the force of mortality μ_x represents the instantaneous rate of transition from alive to dead and is estimated from :

$$\mu_{x,t} = \frac{D_{x,t}}{E_{x,t}}$$

Therefore, despite representing distinct concepts, the two estimations concur. Additionally, the central death rate is a constant for an age x, whereas the force of mortality is usually a function of t for an age x.

Mortality risk and Longevity risk

Mortality risk pertains to the chance of adverse fluctuations in mortality rates, usually concerning an insurance or reinsurance firm. If mortality rates rise unexpectedly, the company might have to pay out more than planned.

On the other hand, *longevity risk* is not a mere reversal of mortality risk; it denotes the risk of individuals living longer than predicted, leading to larger-than-expected mortality improvements. While this is advantageous for the individuals concerned, it can pose financial setbacks for insurance companies or pension funds (Edwards 2020).

Death Rate and Probability of Death

The age-specific death rate is often misunderstood as a vague synonym for the probability of dying. Hereby this misconception is addressed. The latter can be estimated as:

$$q_{i,t} = \frac{D_{i,t}}{N_{i,t}},$$

where $D_{i,t}$ refers to the population aged i in the year t that died inside the age interval of $\{x_i, x_{i+1}\}$ and $N_{i,t}$ represents the population aged exactly x_i (Chiang and Organization 1979).

Identification Issues Lee-Carter

If constraints are not imposed the model will face identification problem. The parameterization

$$(\alpha_x, \beta_x, \kappa_t) \hookrightarrow (\alpha_x, \frac{\beta_x}{c}, c \times \kappa_t)$$

does not uniquely define the estimates, since :

$$\log(m_{x,t}) = \alpha_x + \frac{\beta_x}{c}\kappa_t c + \epsilon_{x,t}$$

produces the same outcome as :

$$\log(m_{x,t}) = \alpha_x + \beta_x \kappa_t + \epsilon_{x,t}$$

Likewise, the same holds for the parameterization:

$$(\alpha_x, \beta_x, \kappa_t) \hookrightarrow (\alpha_x - c\beta_x, \beta_x, \kappa_t + c)$$

Hence, constraints need to be imposed in order to ensure identifiability of the model's parameters.

Lee-Carter Poisson Setting Derivations

Knowing that $D_{x,t} \sim Poisson(E_{x,t}\mu_{x,})$, with probability mass function $Poisson(\lambda) = \frac{e^{-\lambda}\lambda^k}{k!}$ for k= 0, 1, 2, ... , we get :

$$\begin{aligned}
L(\alpha, \beta, \kappa; d) &= \log \prod_x \prod_t \frac{e^{(-E_{x,t}m_{x,t})}(E_{x,t}m_{x,t})^{D_{x,t}}}{D_{x,t}!} \\
&= \sum_x \sum_t \log \frac{e^{(-E_{x,t}m_{x,t})}(E_{x,t}m_{x,t})^{D_{x,t}}}{D_{x,t}!} \\
&= \sum_x \sum_t \log[e^{(-E_{x,t}m_{x,t})}] + D_{x,t} \log (E_{x,t}m_{x,t}) - \log[D_{x,t}!] \\
&= \sum_x \sum_t (-E_{x,t}m_{x,t}) + D_{x,t} \log (E_{x,t}m_{x,t}) - \log[D_{x,t}!] \\
&= \sum_x \sum_t D_{x,t}(\log (E_{x,t}) + \log (m_{x,t}) - E_{x,t}m_{x,t} - \log[D_{x,t}!] \\
&= \sum_x \sum_t D_{x,t}(\alpha_x + \beta_x\kappa_t) + D_{x,t} \log (E_{x,t}) - E_{x,t}m_{x,t} - \log[D_{x,t}!] \\
&= \sum_x \sum_t D_{x,t}(\alpha_x + \beta_x\kappa_t) - E_{x,t}m_{x,t} + c,
\end{aligned}$$

where $c = -\sum_x \sum_t D_{x,t} \log (E_{x,t}) + \log[D_{x,t}!]$.

B Additional Figures

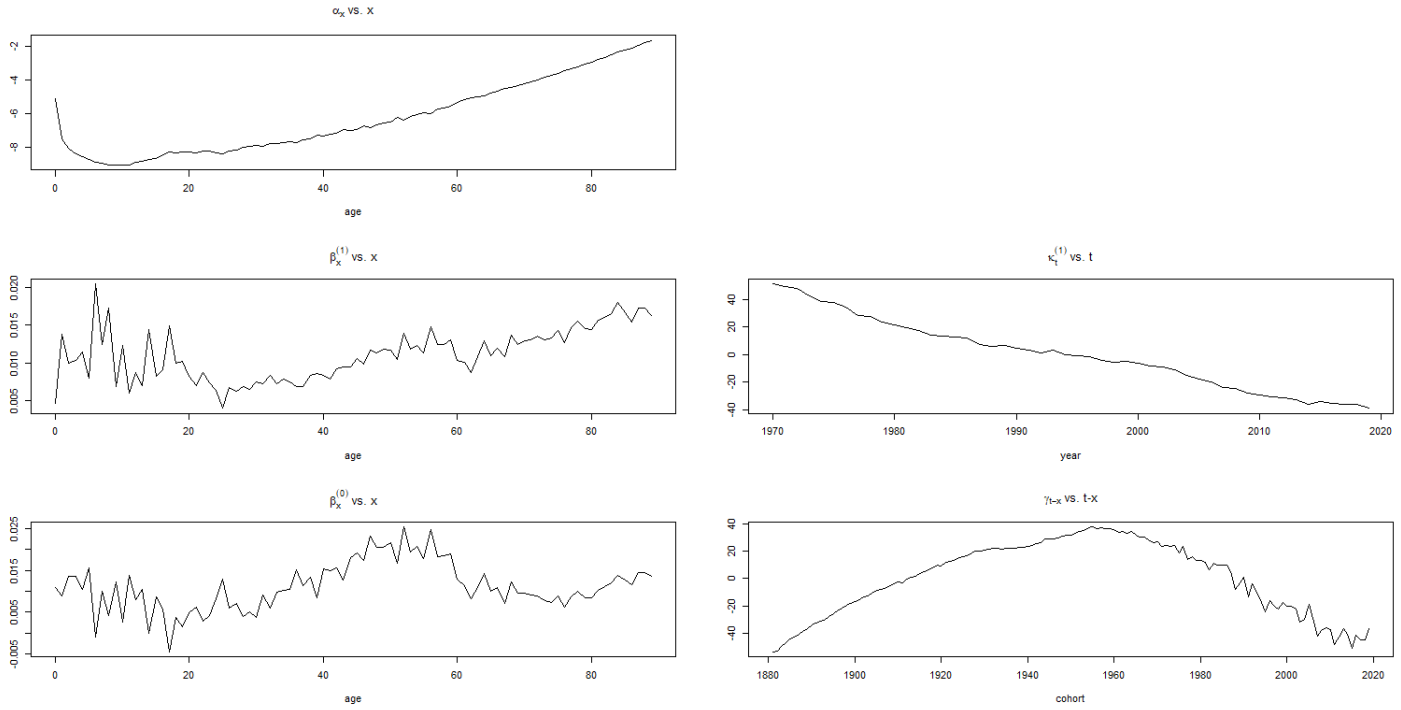

Figure 28: Parameters of RH model for Dutch female population with ages 0-90 for the period 1970-2019.

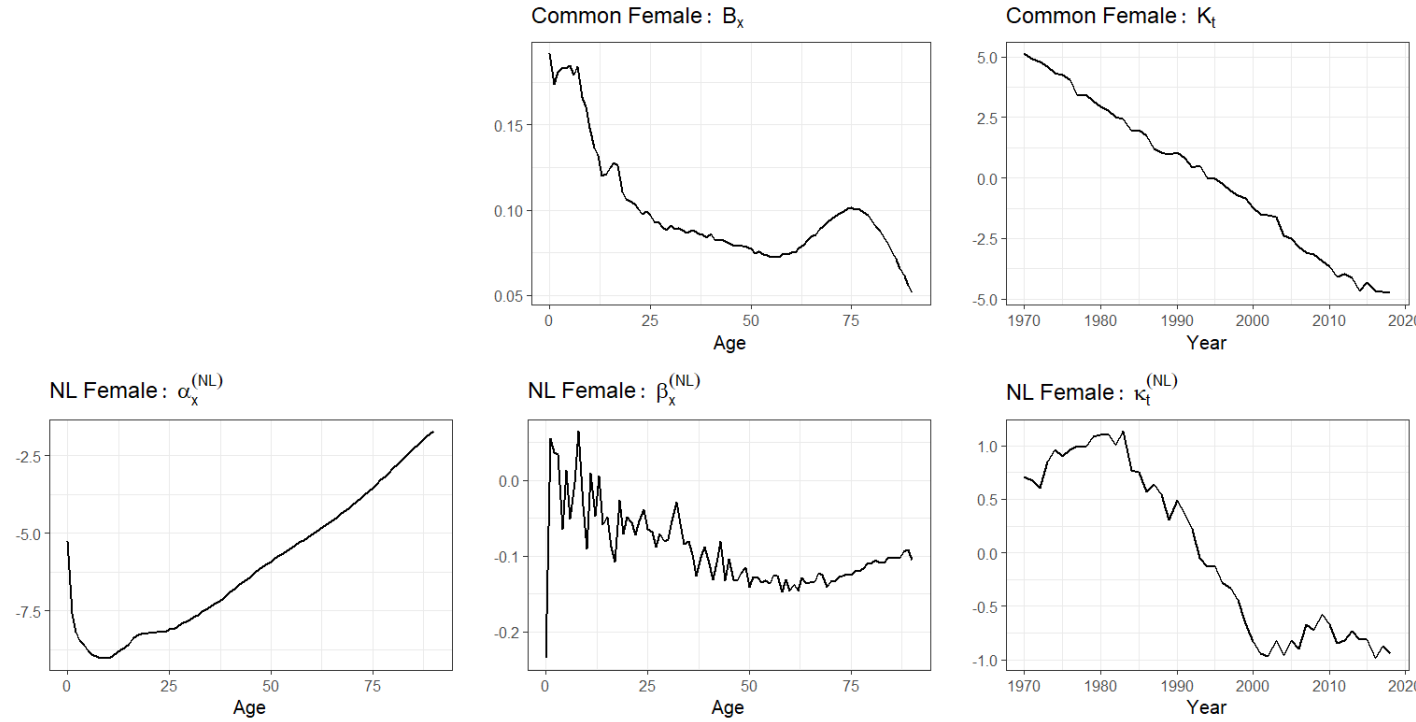

Figure 29: Parameters of LL model for Dutch female population with ages 0-90 for the period 1970-2019.

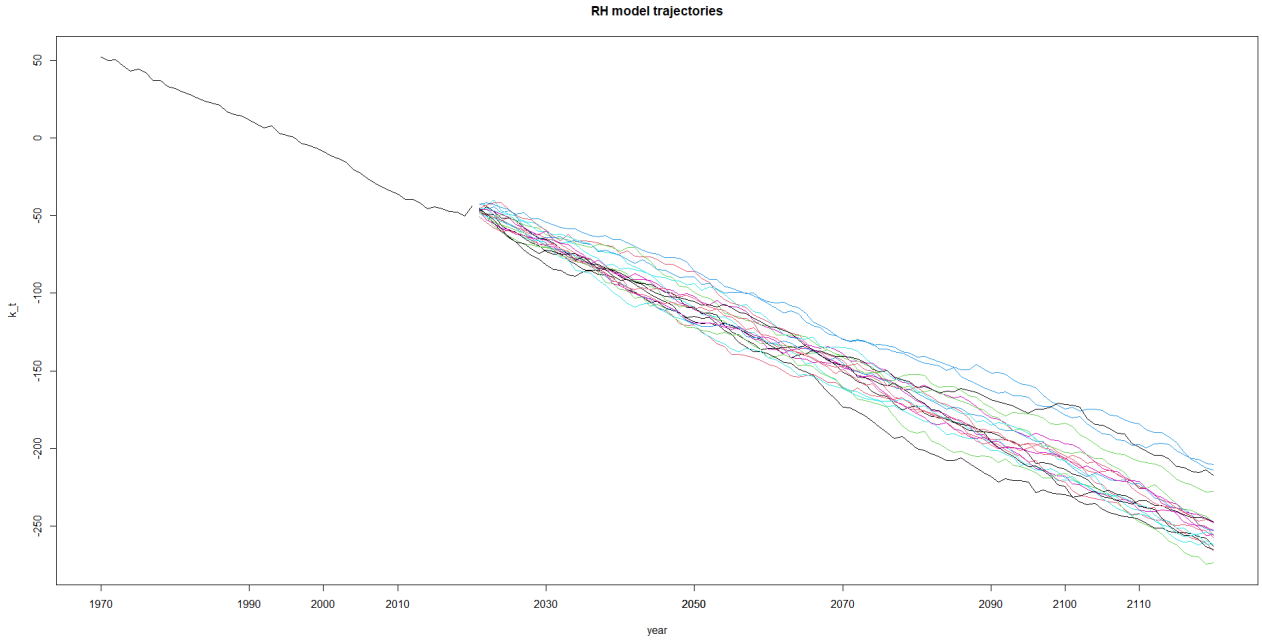

Figure 30: Historical and 20 trajectories for parameter κ_t of the Renshaw-Haberman model

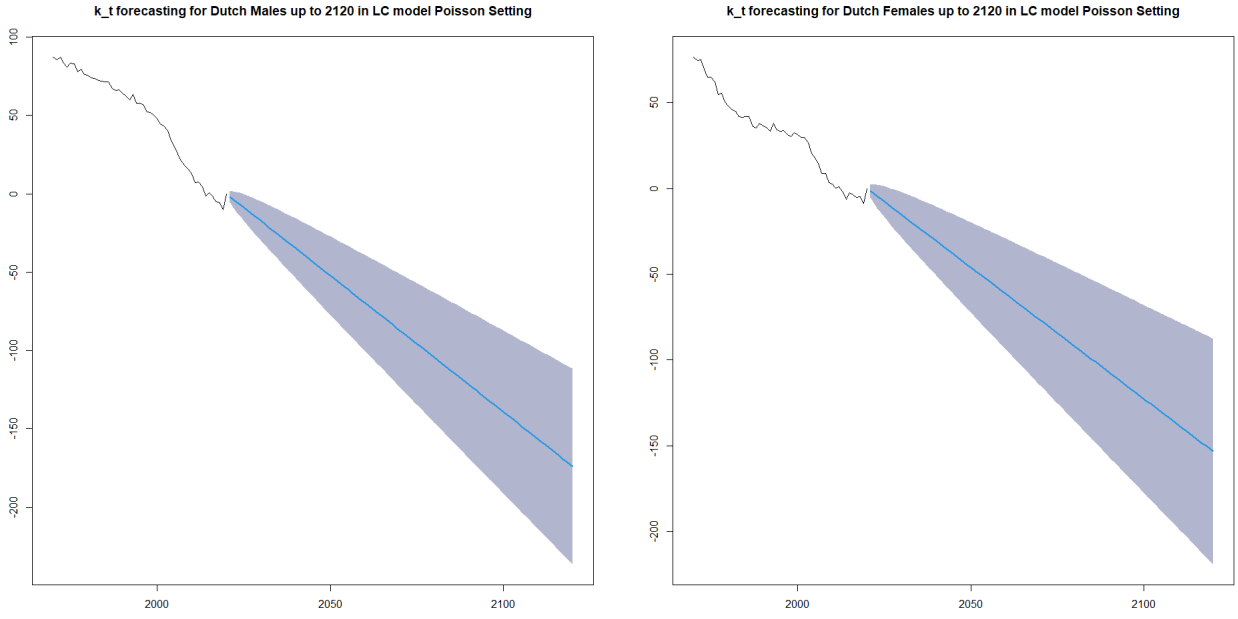

Figure 31: Historical and projected evolution of κ_t in the Lee-Carter Poisson setting

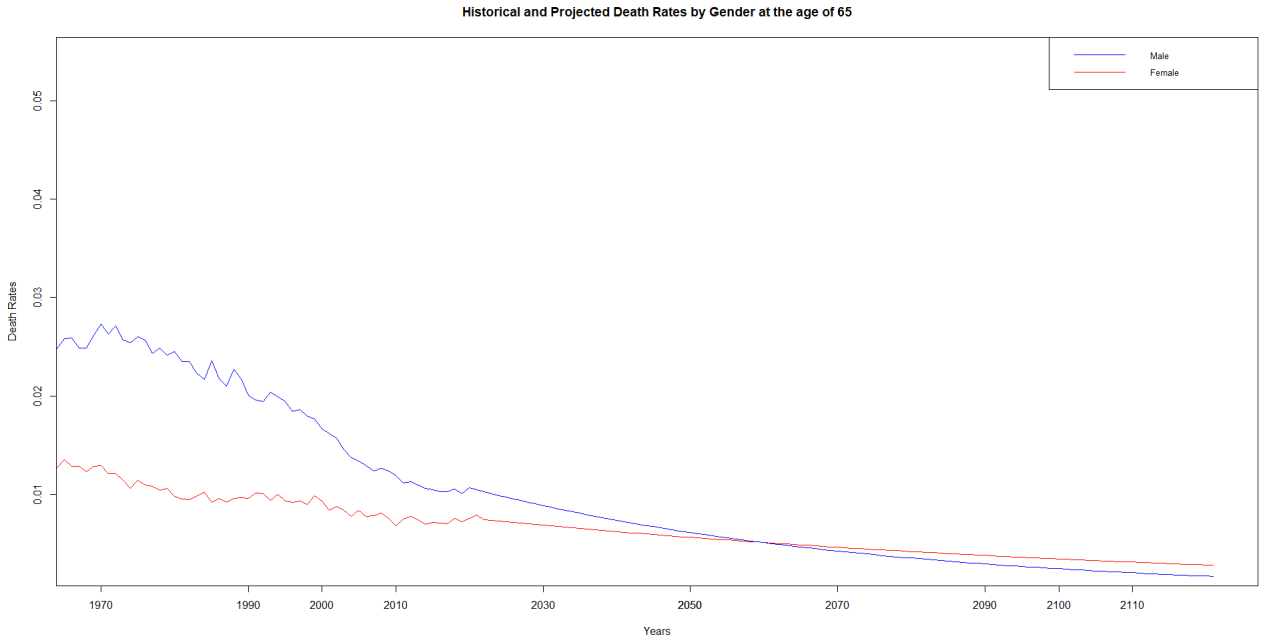

Figure 32: Historical and projected evolution of mortality rates in the Lee-Carter model for Dutch males at the age of 65

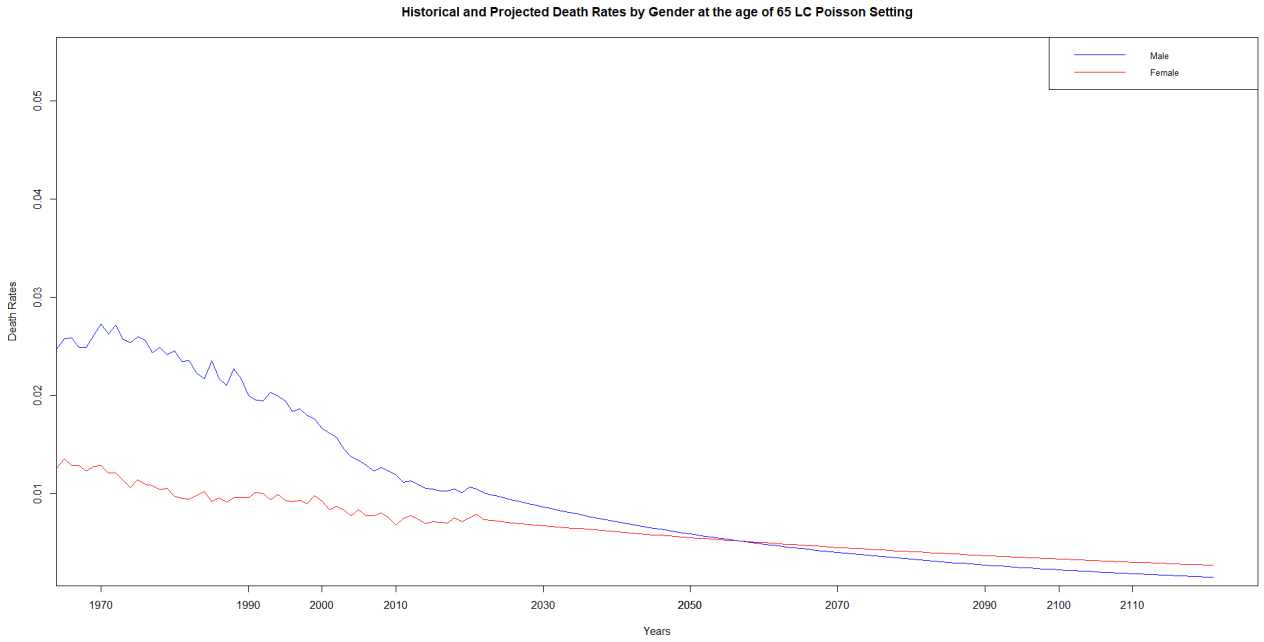

Figure 33: Historical and projected evolution of mortality rates in the Lee-Carter Poisson setting for Dutch males at the age of 65

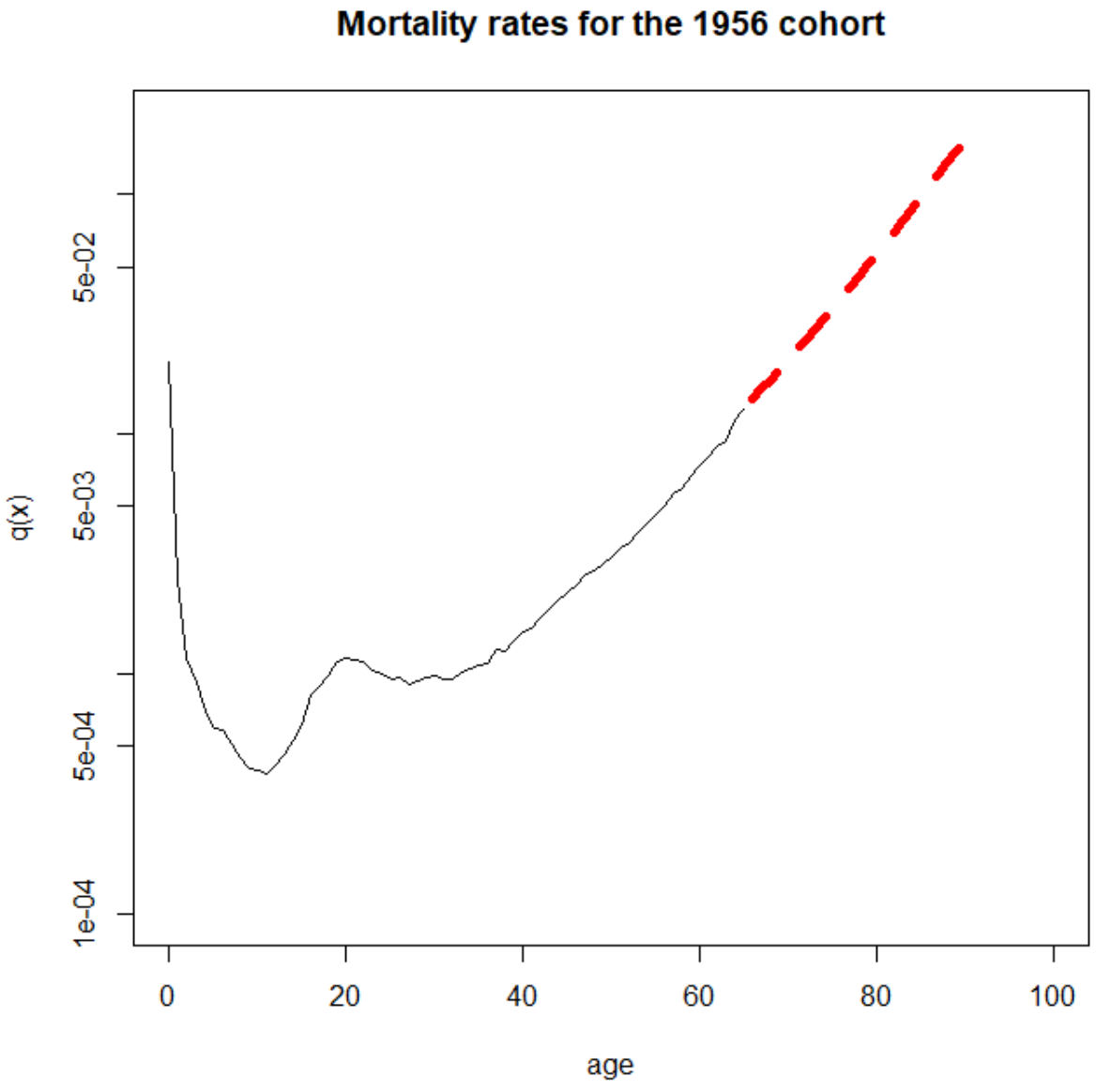

Figure 34: Historical and projected evolution of mortality rates in the Lee-Carter model for Dutch males at the age of 65 (1956 cohort)

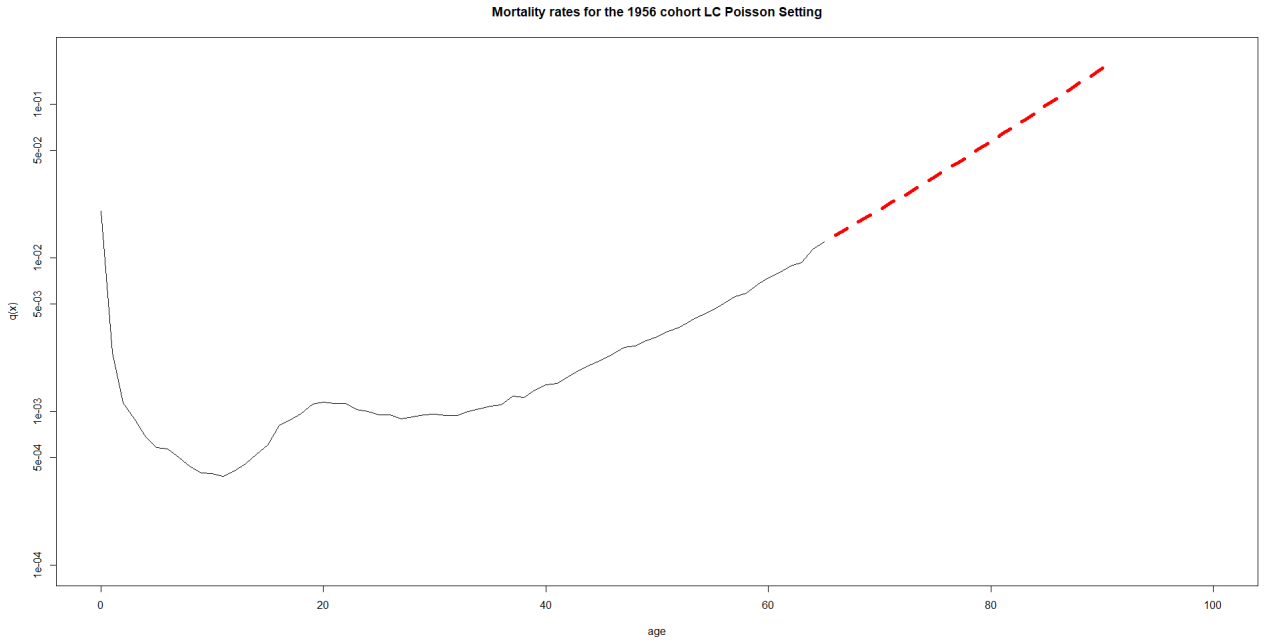

Figure 35: Historical and projected evolution of mortality rates in the Lee-Carter Poisson setting for Dutch males at the age of 65 (1956 cohort)

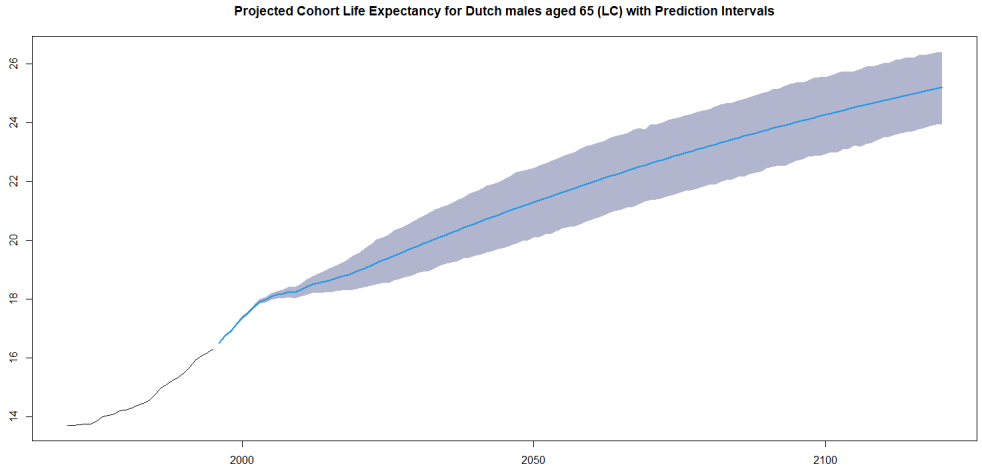

Figure 36: Cohort Life expectancy in LC setting with prediction intervals

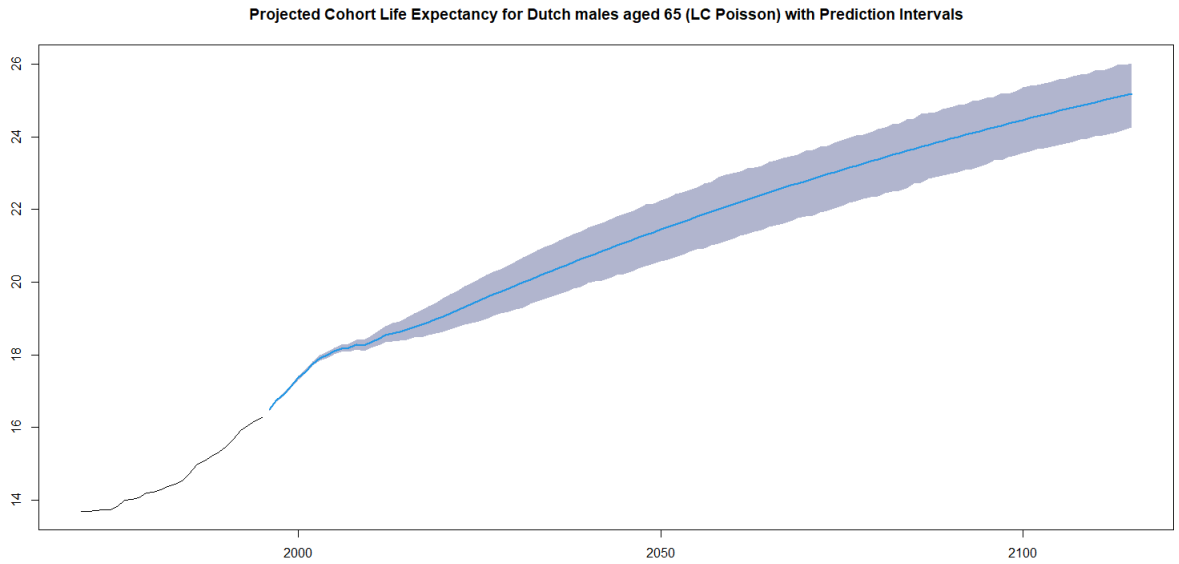

Figure 37: Cohort Life expectancy in LC Poisson setting with prediction intervals

	2021	2022	2023	2024	2025	2026	2027	2028	2029	2030	2031
0	3.852549e-03	3.752973e-03	3.666434e-03	3.569002e-03	3.488115e-03	3.394893e-03	3.309613e-03	3.228039e-03	3.142206e-03	3.073164e-03	2.988384e-03
1	2.368684e-04	2.279855e-04	2.200067e-04	2.112190e-04	2.040998e-04	1.958042e-04	1.892567e-04	1.823866e-04	1.756127e-04	1.696966e-04	1.625912e-04
2	1.480214e-04	1.434394e-04	1.383730e-04	1.357661e-04	1.288197e-04	1.275001e-04	1.204016e-04	1.193828e-04	1.161068e-04	1.122801e-04	1.111435e-04
3	1.308876e-04	1.268024e-04	1.220614e-04	1.176543e-04	1.128409e-04	1.092995e-04	1.045584e-04	1.014194e-04	9.696856e-05	9.324332e-05	8.981183e-05
4	1.353439e-04	1.316992e-04	1.319721e-04	1.263040e-04	1.220424e-04	1.137635e-04	1.138536e-04	1.041852e-04	1.053264e-04	9.601508e-05	9.118856e-05
5	7.521974e-05	7.365118e-05	7.051852e-05	6.653627e-05	6.423648e-05	6.172035e-05	6.037610e-05	5.700294e-05	5.627878e-05	5.286718e-05	5.229509e-05
6	1.098773e-04	1.052052e-04	9.795506e-05	9.515546e-05	9.503894e-05	9.088465e-05	8.770258e-05	8.180512e-05	8.160628e-05	7.479890e-05	7.533336e-05
7	7.300502e-05	7.017071e-05	6.748545e-05	6.496232e-05	6.244684e-05	5.997426e-05	5.768154e-05	5.546003e-05	5.338335e-05	5.127166e-05	4.938005e-05
8	8.305845e-05	8.034383e-05	7.777807e-05	7.481218e-05	7.123249e-05	6.887687e-05	6.727432e-05	6.467973e-05	6.239008e-05	5.944346e-05	5.803492e-05
9	8.513353e-05	8.124760e-05	7.898378e-05	7.691998e-05	7.381008e-05	6.918893e-05	6.719929e-05	6.680093e-05	6.403347e-05	6.184742e-05	5.806225e-05
10	7.641561e-05	7.381169e-05	7.131472e-05	6.900862e-05	6.678704e-05	6.455709e-05	6.227975e-05	6.026117e-05	5.842136e-05	5.646582e-05	5.461031e-05
11	9.501078e-05	9.204189e-05	8.856480e-05	8.537377e-05	8.320438e-05	8.117592e-05	7.850460e-05	7.487480e-05	7.293239e-05	7.202668e-05	6.961343e-05
12	6.393207e-05	6.144879e-05	5.965187e-05	5.878260e-05	5.769343e-05	5.526500e-05	5.281477e-05	5.146567e-05	5.171871e-05	4.960176e-05	4.613867e-05
13	8.122995e-05	7.890906e-05	7.614028e-05	7.408008e-05	7.298280e-05	7.166096e-05	6.895152e-05	6.621487e-05	6.462784e-05	6.471896e-05	6.233485e-05
14	3.034024e-04	2.951122e-04	2.899235e-04	2.893728e-04	2.832451e-04	2.692058e-04	2.578903e-04	2.591165e-04	2.615496e-04	2.541078e-04	2.324070e-04
15	1.469721e-03	1.423136e-03	1.378130e-03	1.369846e-03	1.419289e-03	1.397279e-03	1.273533e-03	1.184995e-03	1.249331e-03	1.333133e-03	1.287052e-03
16	4.227089e-04	3.918608e-04	3.803753e-04	3.692334e-04	3.607922e-04	3.562630e-04	3.472741e-04	3.319743e-04	3.190128e-04	3.163980e-04	3.147631e-04
17	6.801464e-04	6.714004e-04	6.066086e-04	5.888790e-04	5.716845e-04	5.607395e-04	5.590839e-04	5.463064e-04	5.178216e-04	4.948440e-04	4.967841e-04

Figure 38: Forecasted mortality probabilities matrix

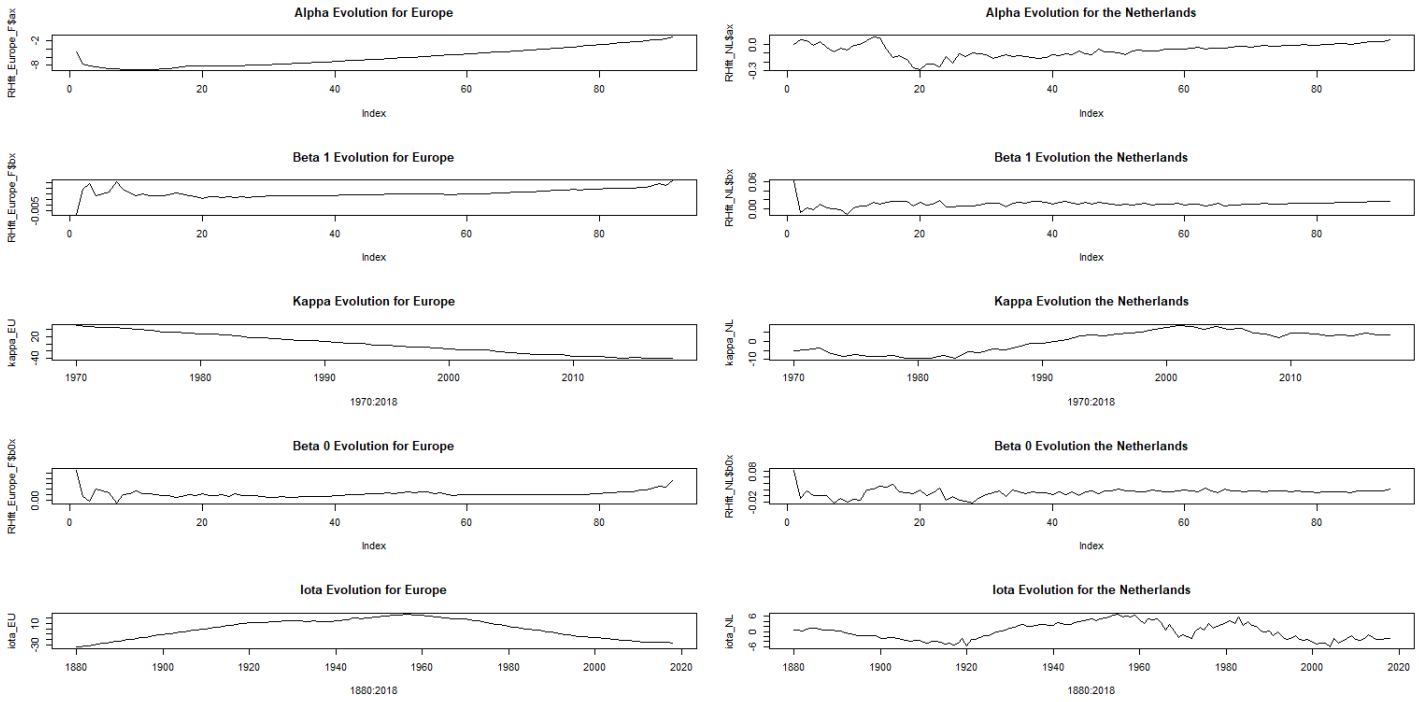

Figure 39: DRH parameters' evolution Dutch females 1970:2018

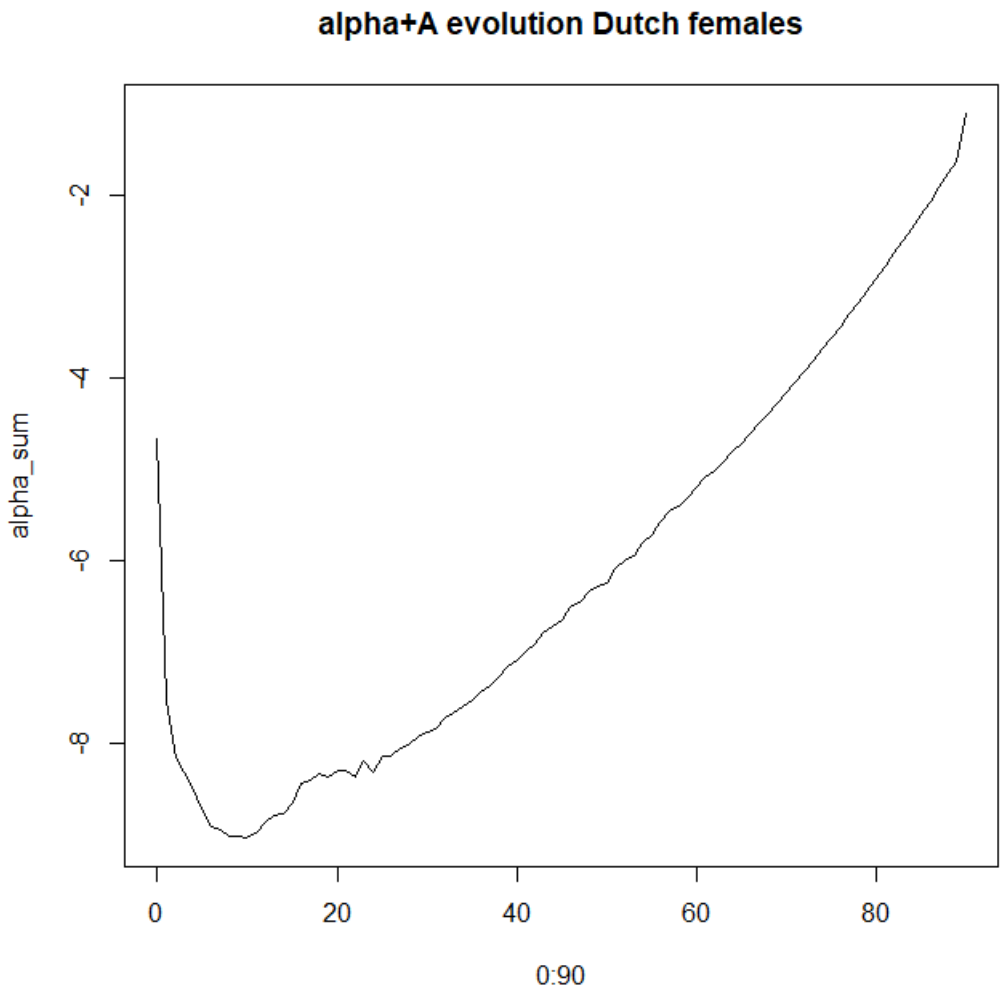

Figure 40: Combined alpha evolution Dutch females

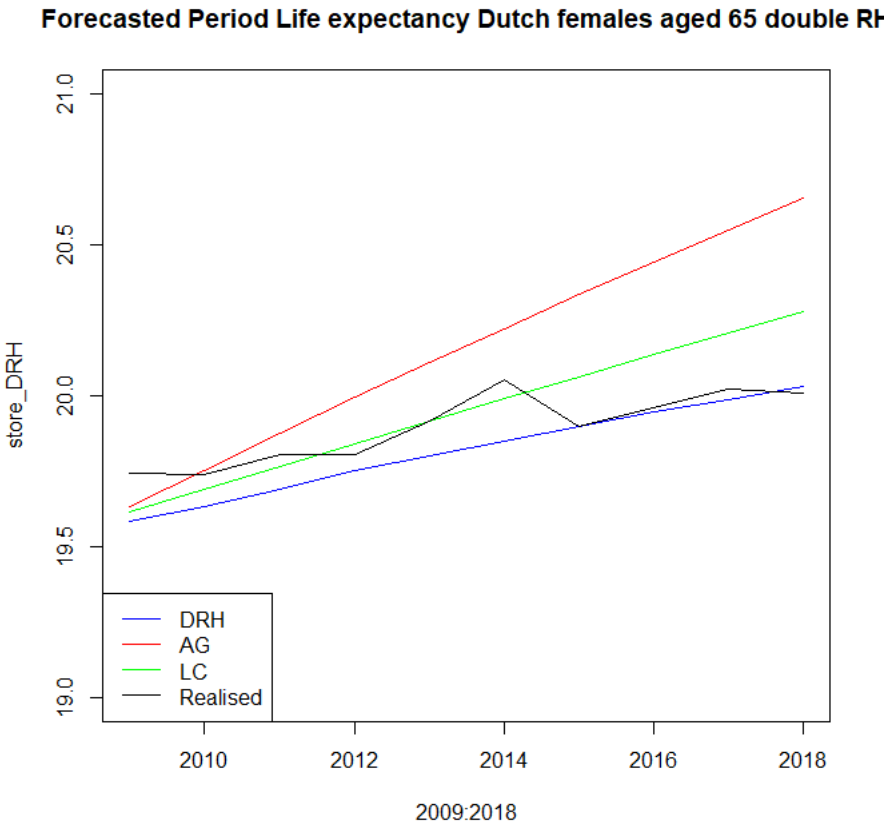

Figure 41: Forecasted period life expectancy for 65 year old females 2009-2018 for DRH, AG, LC.

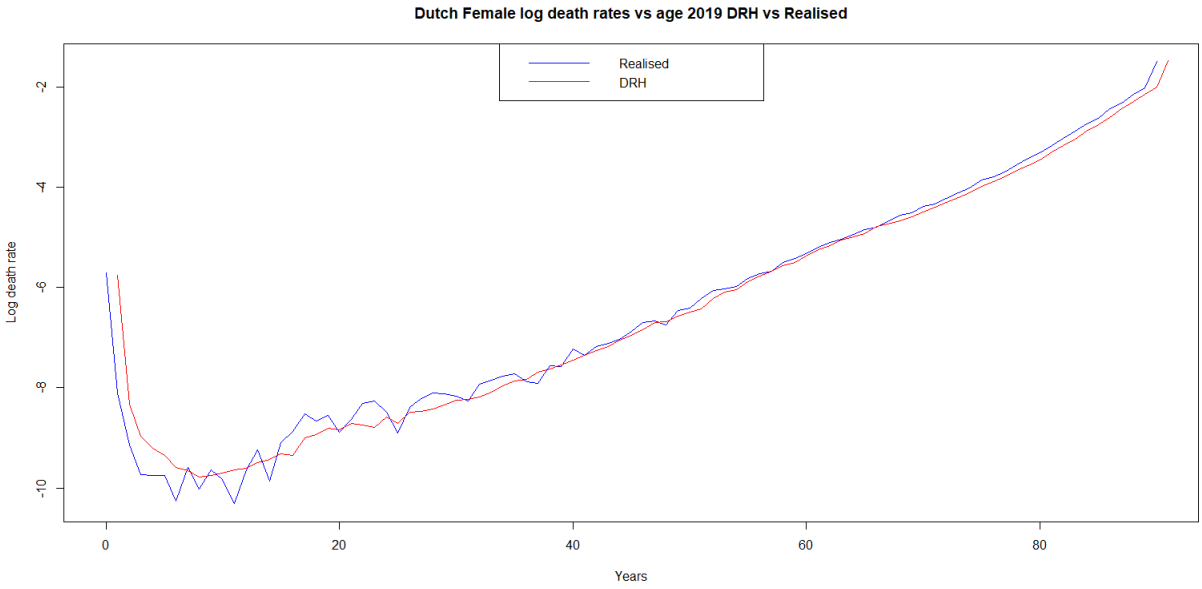

Figure 42: Forecasted evolution of log mortality rates for Dutch females in 2019 against realised rates

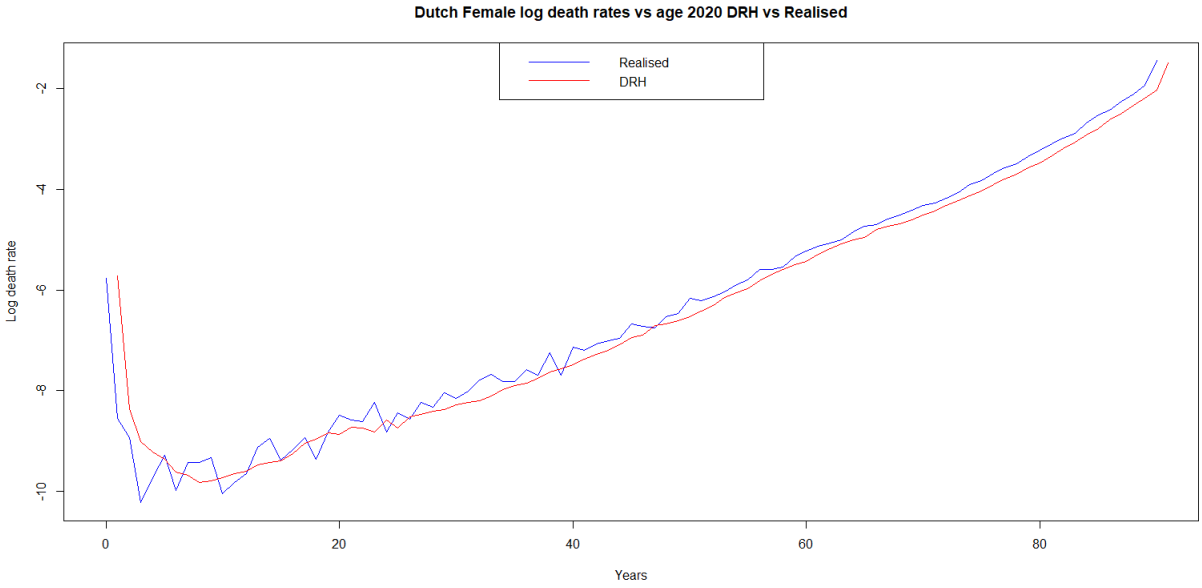

Figure 43: Forecasted evolution of log mortality rates for Dutch females in 2020 against realised rates

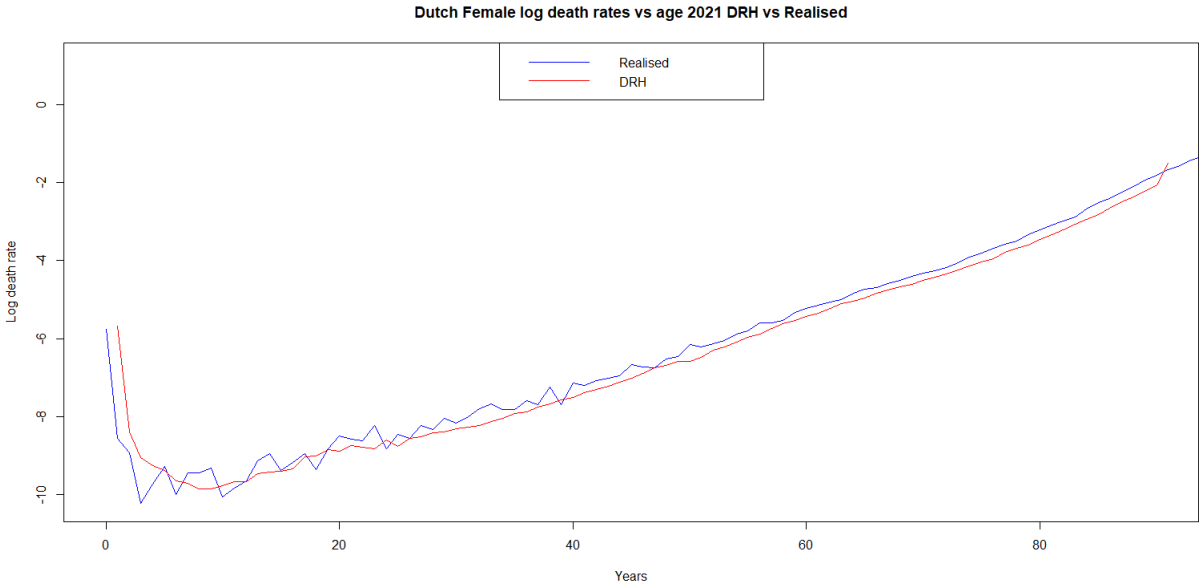

Figure 44: Forecasted evolution of log mortality rates for Dutch females in 2021 against realised rates

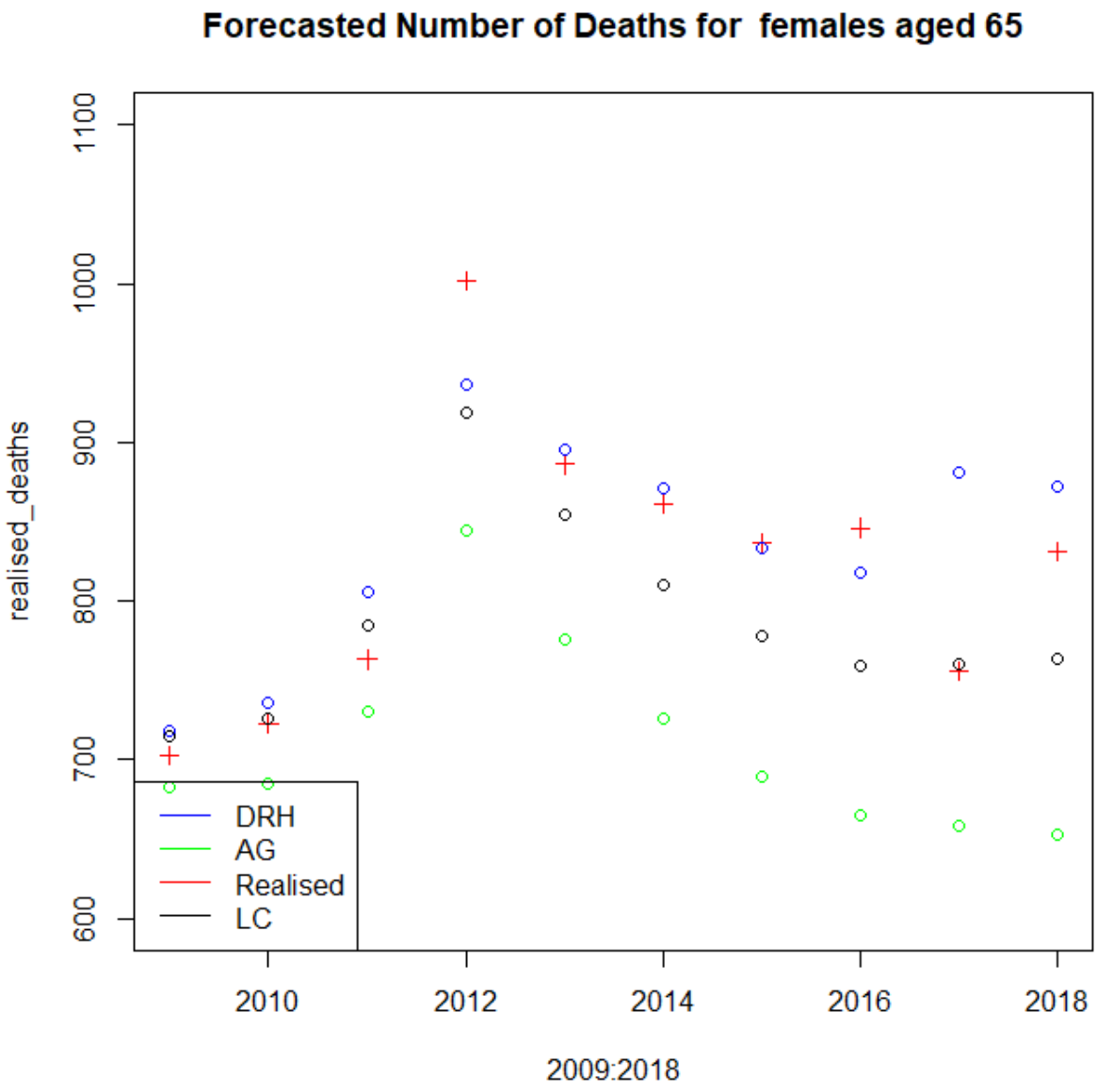

Figure 45: Forecasted number of deaths for 65 year old females 2009-2018 for DRH, AG, LC.

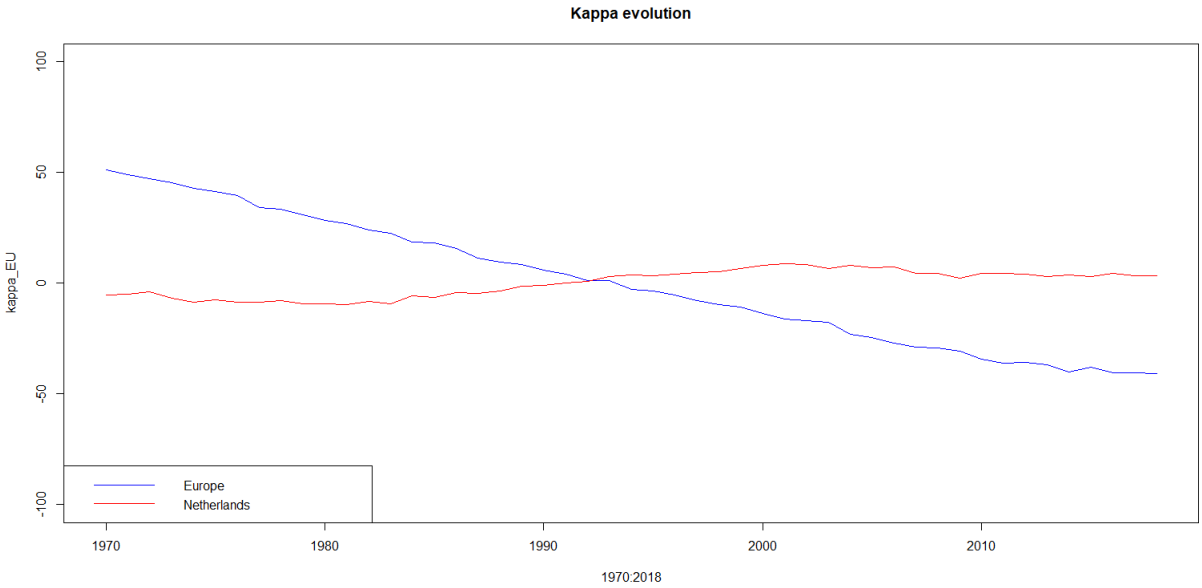

Figure 46: Combined alpha evolution Dutch females